EXPLORATION POTENTIAL AND VARIATIONS IN SHELF PLUME SANDSTONES, NAVARRO GROUP (MAESTRICHTIAN), EAST CENTRAL TEXAS

BY

JOSEPH ELTON PATTERSON, JR., B.A.

THESIS

Presented to the Faculty and Graduate School of

The University of Texas at Austin

in Partial Fulfillment

of the Requirements

for the Degree of

MASTER OF ARTS

THE UNIVERSITY OF TEXAS AT AUSTIN

December 1983

PREFACE

This thesis is written in manuscript form for submittal to the American Association of Petroleum Geologists Bulletin.

ACKNOWLEDGEMENTS

I would like to thank the many people who have helped me in the course of this study. I thank my supervisor, Dr. Alan J. Scott, for suggesting the study and for all of his encouragement and helpful suggestions during its preparation. I also thank Dr. W. E. Galloway and Dr. Thor Hansen, my committee members, and Bill Ambrose for the helpful reviews of the manuscript.

I owe many thanks to Don Chastain and the other employees of the J. A. Leonard, Co. for providing much of the data for the detailed study area and to the staff of the Texas Department of Water Resources for their courteous aid in obtaining well log data for the regional study area. Thanks are also due Mr. Robert Grayson for providing well logs for the regional study area.

Special thanks are owed to Harold Billman and Linda Soar for their invaluable aid in paleobathymetric determinations and to Terry Mulhollan for helping type parts of this work.

Thanks are also due to Scott's 'Dirty Dozen' for all of their aid and moral support through trying times. And finally, I wish to express my deepest thanks to my parents for all their support.

EXPLORATION POTENTIAL AND VARIATIONS IN SHELF PLUME SANDSTONES, NAVARRO GROUP (MAESTRICHTIAN), EAST CENTRAL TEXAS

by Joseph Elton Patterson, Jr.

ABSTRACT

Fine-grained sandstones within the Kemp Clay of the Navarro Group (Maestrichtian) of east central Texas were deposited on a shallow marine shelf by migrating sand-bars. These sands were introduced onto the muddy shelf by coastal/shelf currents which were deflected seaward by prominent deltaic headlands. The injection of terrigenous material, in traction, into this current flow field resulted in the formation of arcuate belts of thin (3-20 ft; 1-6 m) shelf 'sand-plumes' which were 17 to 20 mi (22 to 30 km) wide and extended 27 to 30 mi (44 to 46 km) downdrift and 21 to 40 mi (34 to 64 km) into the basin. Ridges, formed by the stacking of individual bars within the shelf sand-plume, display a change in their long axis orientations (from dip- to strike-oriented downdrift) which corresponds to the flow directions of the deflected shelf currents.

Southwestward, fair-weather reworking of these delta-supplied sands by shelf currents resulted in the down-current stratigraphic climbing of the migrating shelf-bar complexes. Onshore stratigraphic climbing in the landward portions of the plume complexes is believed to be due to storm activity and/or transgressive marine processes. Current patterns, and the resulting distribution of sand, were influenced by the general configuration of the shelf and the topographic relief inherited from previously deposited shelf/slope systems.

Three variations of the basic shelf sandstone-plume model were recognized in the study area: (1) a rapidly deposited, immature shelf sandstone-plume which is high in shale content and number of shale breaks due to insufficient current-winnowing, (2) an abandoned, current reworked shelf sandstone-plume which has a complex depositional history due to shifts in the depositional axis and current modification of the original plume deposits, and (3) a transgressed shelf sandstone plume which exhibits morphologic and lithologic variations as the result of storm reworking and transgressive marine processes. Each of these variants displays unique characteristics which influence their potential as hydrocarbon reservoirs.

TABLE OF CONTENTS

LIST OF TABLES

LIST OF ILLUSTRATIONS

Figure | Page

INTRODUCTION

Upper Cretaceous deposits in the East Texas Basin are dominated by thick (1000-2500 ft; 300-750 m) marine mudstones. Encased in these mudstones are elongate (1 to 6 mi; 1.5 to 10 km), thin (5 to 15 ft; 1.5 to 4.6 m) fine-grained sandstone lenses. Despite their relatively small size and their fine texture, these sandstones have proven to be locally significant hydrocarbon reservoirs within the regional study area (Fig. 1). From their first discovery in 1921 to 1982, cumulative oil production from the Navarro 'A' and 'B' sandstones (Fig. 2), has exceeded 11.5 million barrels (Texas Railroad Commission-1982 Petroleum Production Figures). Even during the economic slow down of the early 1980s, exploration and production drilling remained economically feasible due to the shallow depth (2000-4000 ~~ft~~ m, 6,500-13,100 ~~km~~ ft.) and the fairly prolific nature of the stratigraphically isolated sandstones. Although not a major target for large companies, smaller independent operators have conducted an active exploration program in these upper Cretaceous sandstones.

Earlier studies of the Upper Cretaceous deposits of the East Texas Basin have primarily concentrated on age determinations based on the diverse and abundant micro- and macrofossil assemblages (Hill, 1901; Adkins, 1933; Stephenson, 1941; Pessagno, 1969). Previous attempts to delineate or interpret depositional systems within the Navarro Group, with the notable exception of McGowen and Lopez (1983), have been of a very cursory nature. This paper will present evidence supporting the shallow marine interpretation of these sandstones and will relate their areal

FIGURE 1. - Regional study area location and structural setting. The study area lies at the southwesternmost extent of the East Texas Basin. The paleoshoreline trend roughly parallels the Luling-Mexia-Talco and Balcones fault zones.

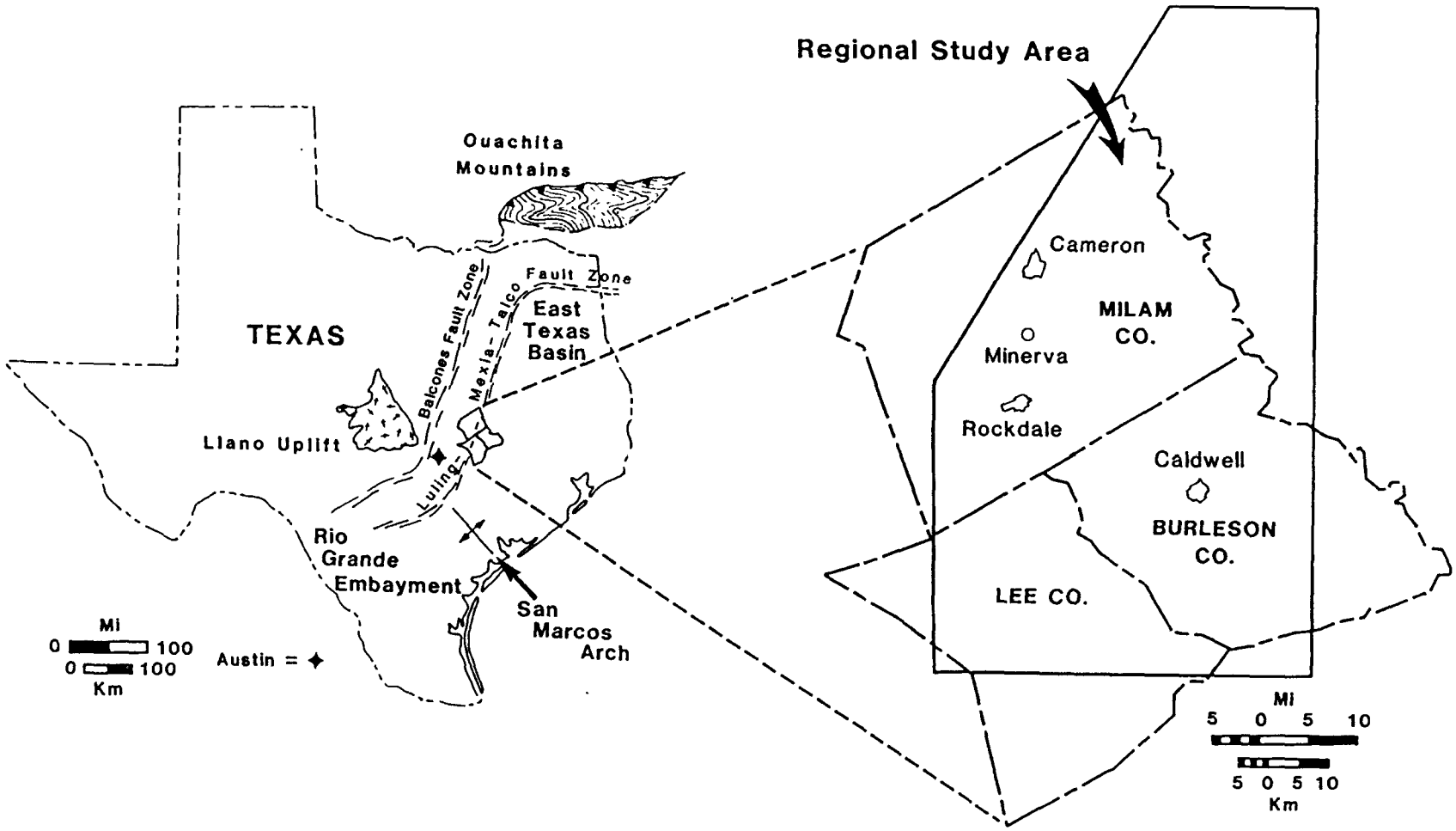
Regional Study Area
Ouachita Mountains
TEXAS
Balcones Fault Zone
Mexia-Talco Fault Zone
East Texas Basin
Llano Uplift
Luling
Rio Grande Embayment
San Marcos Arch
Austin
Mi
0 100
0 100
Km
Cameron
MILAM CO.
Minerva
Rockdale
Caldwell
BURLESON CO.
LEE CO.
Mi
5 0 5 10
5 0 5 10
Km

FIGURE 2. - Upper Cretaceous stratigraphic nomenclature and relationships of northeast, east central and southwest Texas. The Navarro 'A' and 'B' sandstone intervals are located within the Kemp Clay in Milam, Burleson, and Lee Counties.

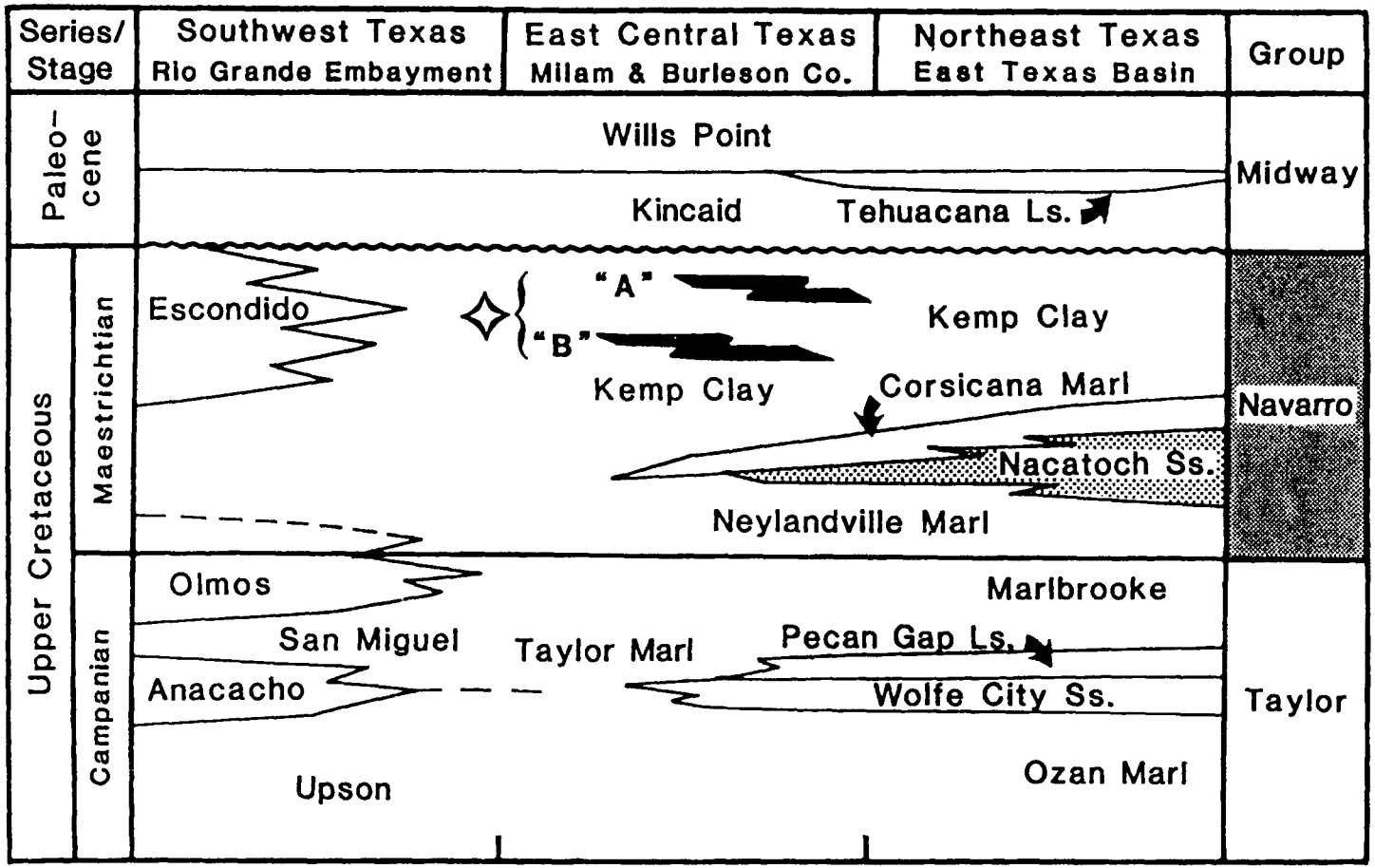
Series/ Stage
Southwest Texas
Rio Grande Embayment
East Central Texas
Milam & Burleson Co.
Northeast Texas
East Texas Basin
Group
Paleo-cene
Wills Point
Midway
Kincaid
Tehuacana Ls.
Upper Cretaceous
Maestrichtian
Escondido
"A"
"B"
Kemp Clay
Kemp Clay
Corsicana Marl
Navarro
Nacatoch Ss.
Neylandville Marl
Campanian
Olmos
Marlbrooke
San Miguel
Taylor Marl
Pecan Gap Ls.
Anacacho
Wolfe City Ss.
Taylor
Upson
Ozan Marl
THIS STUDY

distribution and component facies to the depositional processes active on the mud-rich, late Cretaceous shelf.

Regional Study Area and Stratigraphic Nomenclature

The regional study area is located approximately 30 to 90 miles (50-145 km) northeast of Austin, Texas in Milam, Burleson and Lee Counties and includes approximately 2160 square miles (5594 km^2) (Fig. 1). The area of interest is at the southwesternmost margin of the East Texas Basin and is bounded to the northwest and west by the stable Central Texas Platform, which served as a low relief source area for the Navarro terrigenous clastics, and to the southeast by the Gulf Coast Province that was a shallow marine basin during the Maestrichtian. It is cross-cut by the southwest-northeast trending Luling-Mexia-Talco Fault Zone. To the southwest lies the San Marcos Arch, the structural flexure which separates the East Texas Embayment from the Rio Grande Embayment (Fig. 1).

The Navarro Group in the East Texas Basin is divided into four formations: 1) the Neylandville Marl, which unconformably overlies the Taylor Group (Campanian), 2) the Nacatoch Formation, 3) the Corsicàna Marl and 4) the Kemp Clay (Pessagno, 1969). Unconformably overlying the Kemp Clay is the Tertiary Kincaid Formation of the Midway Group (Stephenson, 1933 and 1941; Pessagno, 1969). An alternative set of nomenclature for subsurface work proposed by Nichols, et al,(1968) and modified by Kreitler, et al, (1980 and 1981) is summarized in Table 1.

The formation of interest in this study is the Kemp Clay of Stephenson (1941) which is referred to as the Upper Navarro Clay by Kreitler, et al, (1980 and 1981). These marine shales are of mid-

Table 1 - Comparison of Stratigraphic Nomenclature

	This Study	Kreitler et.al. (1980, 1981)	Pessagno (1969)	Nichols et.al. (1968)
Navarro Group	Kemp Clay: Navarro "A" / Navarro "B"	Upper Navarro Clay	Kemp Clay	Upper Navarro
	Corsicana Marl	Upper Navarro Marl	Corsicana Marl	
	Nacatoch Sandstone	Nacatoch Sand	Nacatoch Sand	Nacatoch Sandstone
	Neylandville Marl	Lower Navarro	Neylandville Marl	Lower Navarro

Maestrichtian age (Pessagno, 1969) and were deposited during the waning stages of the major late Cretaceous transgression of the North American continental interior (Vail, 1977). Wells drilled in the regional study area contain two distinct sandstone intervals within the Kemp Clay (Upper Navarro Clay). Locally, petroleum explorationists refer to the uppermost of these zones as the Navarro 'A' and the older interval as the Navarro 'B' (lower) sandstone (Figs. 3 and 4). This informal terminology will be used in the present study.

To facilitate the study of the Navarro 'A' and 'B' intervals, genetic subunits were delineated on the basis of well log responses of the intervals and resistivity and conductivity characteristics of the interbedded shales (Fig. 4). The lower of the sandstones, the Navarro 'B' interval, is divided into four subunits designated B1 through B4 in ascending order. Delineation of these subdivisions was made possible by the presence of laterally persistent interbedded shales and the dense well control in the detailed area (Fig. 5). The Navarro 'A' interval is likewise divided into three subunits denoted as A1 through A3 in ascending order (Fig. 4).

SHELF PROCESSES AND SANDSTONES

Siliciclastic shelf-sandstones and the processes which govern their accumulation have received increasing attention by researchers in recent years. This is due to the recognition of their importance as hydrocarbon reservoirs and the potential of stratigraphic traps associated with such sandstones. As knowledge of these shelf sand bodies has increased, so has the realization that they may form under a variety of conditions and are influenced by various shelf processes.

FIGURE 3. - Regional type electric log showing major groups and formations. The Navarro 'A' and 'B' sandstone intervals have been designated.

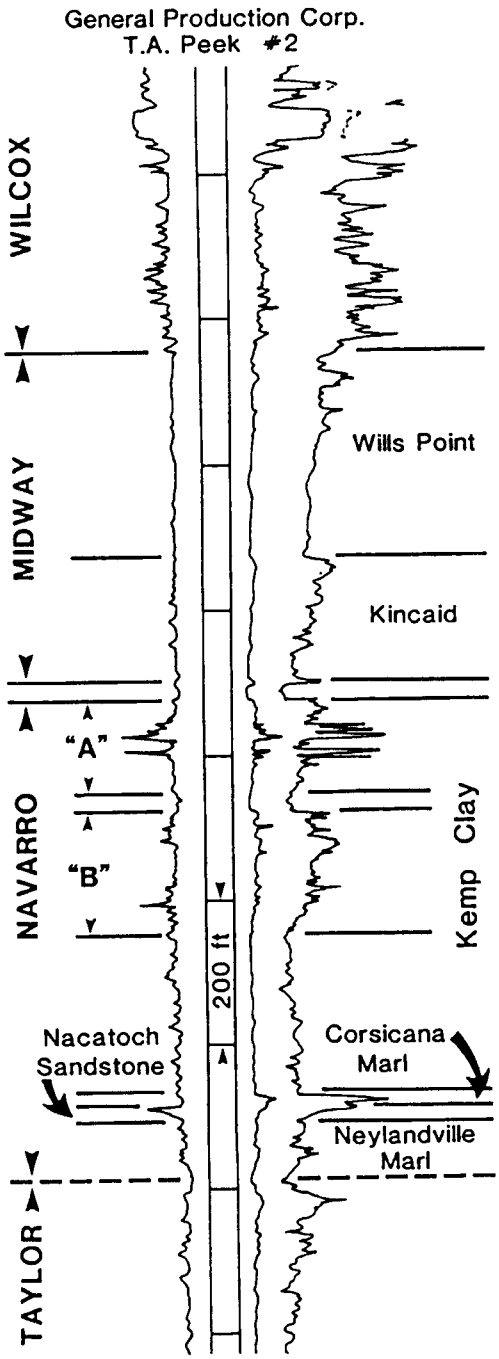
General Production Corp.
T.A. Peek #2
WILCOX
MIDWAY
NAVARRO
TAYLOR
"A"
"B"
200 ft
Wills Point
Kincaid
Kemp Clay
Nacatoch
Sandstone
Corsicana
Marl
Neylandville
Marl

FIGURE 4. - Detailed type electric log showing genetic subunits and shale markers.

J.A. Leonard – Flentge #1

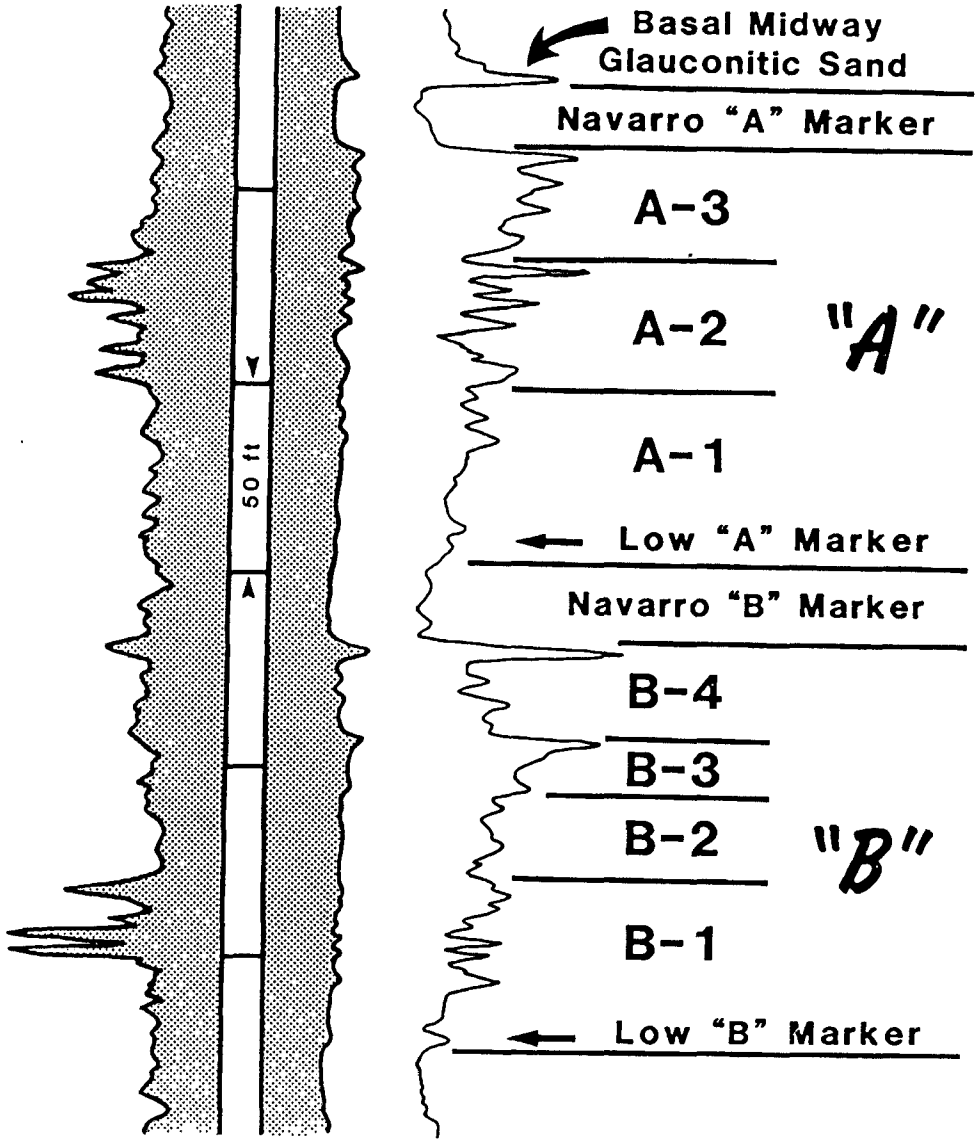

FIGURE 5. - **A.** Regional well control and Navarro outcrop pattern. **B.** Well control for detailed study area. Shown are locations for type electric logs (large circles) and cores used for paleobathymetric determinations (triangles). See Fig. 11 for detailed cross-sections C-C' and D-D'.

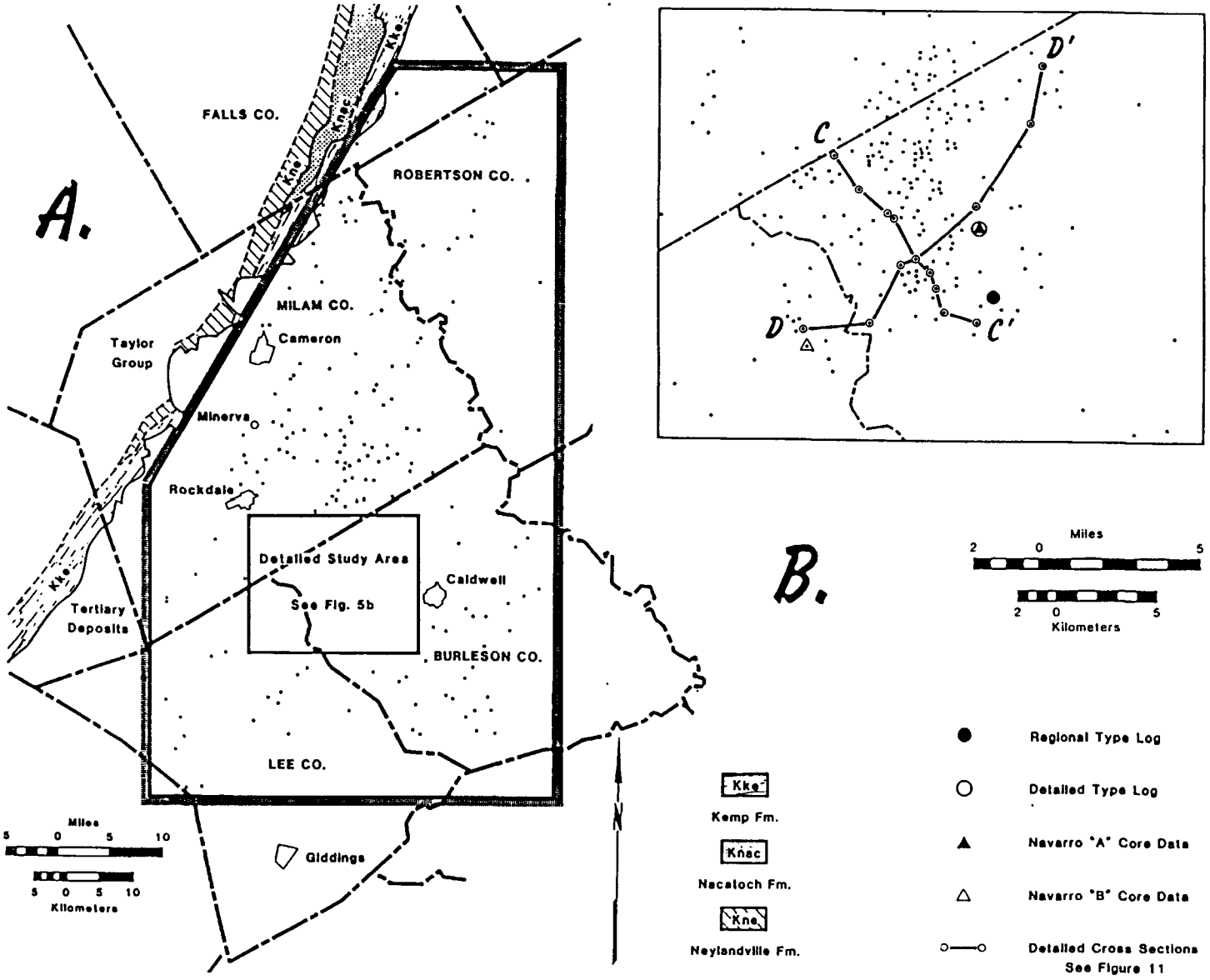
A.
FALLS CO.
ROBERTSON CO.
MILAM CO.
Cameron
Taylor Group
Minerva
Rockdale
Detailed Study Area
See Fig. 5b
Caldwell
BURLESON CO.
LEE CO.
Giddings
Tertiary Deposits
Kke
Knac
Kne
Miles
5 0 5 10
5 0 5 10
Kilometers
B.
C
C'
D
D'
Miles
2 0 5
2 0 5
Kilometers
Kke
Kemp Fm.
Knac
Nacatoch Fm.
Kne
Neylandville Fm.
Regional Type Log
Detailed Type Log
Navarro "A" Core Data
Navarro "B" Core Data
Detailed Cross Sections
See Figure 11

Modern Shelf Processes

Much of the early investigation of modern shelf sands focused on areas such as the southern North Sea and the seas around the British Isles. These studies concentrated on the effects of strong tidal action on transgressed relict sand deposits of the shallow European continental shelf. Numerous workers have contributed to the understanding of process-response relationships in these tide-influenced shelf environments including Stride (1963), Belderson and Stride (1966), Houbolt (1968), Kenyon (1970), Terwindt (1971), McCave (1971), Caston (1972) and Anderton (1976).

The North American Atlantic shelf off the southeastern coast of the United States has also been intensively studied. As with the North Sea shelf sands, the sand forming the ridges and shoals of Atlantic shelf are derived from transgressed and reworked relict Pleistocene deposits. The primary processes involved in this reworking, however, are wave and storm generated current action as documented in the studies of Pilkey and Field (1972), Swift (1975), Swift, et al, (1971, 1972, 1973 and 1977), Field (1980), Swift and Field (1981) and Pilkey, et al, (1981).

Oceanic currents which move along continental margins may intrude onto the shelves with sufficient energy to transport significant volumes of sand-sized sediment (Flemming, 1980 and 1981). The influence of shelf configuration on unidirectional shelf currents was considered by McManus and Creager (1963). Other studies have emphasized storm-generated currents as a mechanism for transporting sediments onto the shelf (e.g. Hayes, 1967; Hamblin and Walker, 1979; Field, et al, 1981).

The effect of shoreline morphology on coastal/shelf current fields and the resultant sediment dispersal patterns has been documented by Coleman et al, (1981) for an area of the Sinai shelf adjacent to the Nile River delta. Measurements of currents in the vicinity of the eastern portion of the Nile delta indicate that eastward flowing coastal/shelf currents are deflected basinward by the prominent, cuspate, deltaic headland formed by the Damietta distributary. The areal distribution of sand and sand wave bedforms, as determined from side-scan sonar and bottom samples, document the injection of sediment from the this distributary into the coastal current system. These sediments are transported as bedload north and eastward onto the Sinai shelf forming a distinct plume-like sand body. The shelf sand-plume is a belt of migrating sandy bedforms 3-12 miles (5-20 km) wide which extends at least 30 miles (50 km) offshore and to within 6-9 miles (10-15 km) of the shelf break. These shelf sands, which were deposited in water depths of 75-180 feet (25-60 km), form an arcuate, 'plume-like' pattern basinward and downcurrent from their deltaic source area. On the protected, down-current side of the deltaic headland, an entrapped eddy system provides a quiescent environment for the deposition of silt and clay. A simplistic analogy of this type of system is illustrated in figure 6. Figure 6a represents a vertical cross-section through a sand wave and the current flow fields associated with the bedform while figure 6b is a plan view of a deltaic headland with its accompanying coastal and shelf current patterns. Current flow paths are deflected around the upcurrent side of the two features and achieves flow separation near the apex. Entrained sediment is carried away from the distributary mouth in an arcuate path downcurrent from the deltaic headland.

Late Cretaceous Shelf Sandstones

Shelf deposits have been recognized in a variety of basins and settings. Late Cretaceous shelf sandstone deposits have been described by numerous workers in the Western Interior seaway including Berg (1975), Porter (1976), Spearing (1976), Brenner (1978), Boyles and Scott (1982), Hobson et al, (1982), and Porter and Weimer (1982) to name but a few. Similar late Cretaceous shelf sandstones have been documented in the East Texas basin by McGowen and Lopez (1983) and Turner and Congers (1981).

The shelf sand-plume concept (Coleman, et al, 1981) has been utilized by Palmer and Scott (in press) to explain the distribution of shelf sandstones in the La Ventana Tongue of the Cliff House Sandstone (Campanian) from the San Juan Basin of New Mexico. Several prominent arcuate basinward bulges in net sandstone distribution maps correspond to the depositional axes of delta-attached shelf sandstone 'plumes'. In areas of dense well control, these sandstones can be traced 20-30 miles (32-48 km) down-paleocurrent and extend 5-15 miles (8-24 km) offshore of the inferred paleoshoreline.

The plume model has been further developed by Barratt (1982) in his investigation of the Fales Sandstone (Campanian) in the Wind River Basin of Wyoming. Subsurface mapping of lithofacies relationships was made possible by the availability of several closely spaced cores from the West Poison Spider Field. This detailed lithologic data permitted the recognition of multiple genetic units within the Fales Sandstone. Transgression of the deltaic/shelf system resulted in disruption of the current flow fields which created the shelf sand-dispersal system. The sand plume was reworked by

storm waves and bars migrated onshore in a manner similar to the shelf-bars of the Duffy Mountain sandstone described by Boyles and Scott (1982). Continued transgression preserved the resultant Fales shelf-bars in a blanket of marine shale.

OBJECTIVES AND METHODS

The primary objectives of this study are to continue the development of the shelf sand-plume concept by documenting the detailed anatomy of two Kemp Clay (Upper Navarro Clay) shelf sandstone complexes and to describe three major plume types. To facilitate description of these shelf systems, a generalized shelf sand plume is depicted, with its various component areas labelled, in figure 6c. Occurrence of these thin shelf sandstones within a mud-rich sequence, as well as the availability of sufficient subsurface control, has permitted the Navarro 'A' and 'B' sandstone intervals to be divided into several mappable subunits (Figs. 3 and 4). Detailed examination of the geometries, lateral trends and stratigraphic relationships of the subunits has been used to document the depositional history of these shelf sandstones. Using this information we will 1) propose a depositional model for an idealized Navarro shelf sandstone-plume, 2) describe three major variants based on the reconstructed depositional history of specific sandstone intervals and 3) suggest qualitative estimates of hydrocarbon potential for the various component zones of each of these shelf plume types.

Description of the Navarro 'A' and 'B' sandstones is based on a total of 391 electric, induction electric, dual-induction and gamma-ray logs were

FIGURE 6. - **A.** Vertical cross-section of sand wave showing current flow fields. Note flow separation at crest and zone of backflow and eddying on lee side. **B.** Schematic plan view of current flow fields associated with deltaic headland and resulting sand dispersal pattern. **C.** Idealized morphological divisions of shelf sand-plume for use as references for discussion.

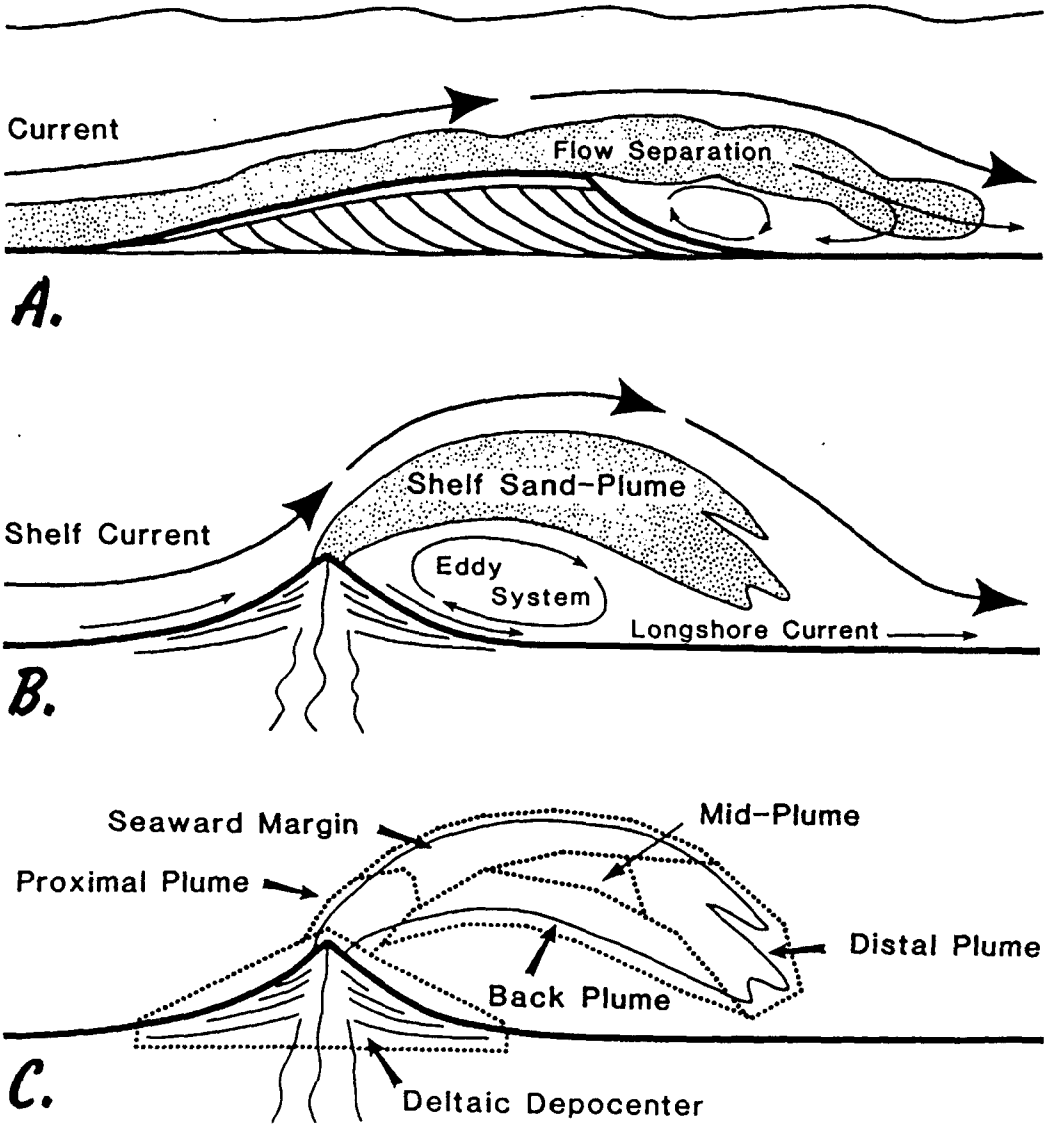
Current
Flow Separation
A.
Shelf Current
Shelf Sand-Plume
Eddy
System
Longshore Current
B.
Seaward Margin
Mid-Plume
Proximal Plume
Distal Plume
Back Plume
C.
Deltaic Depocenter

obtained from a 2160 square mile regional study area (Fig. 5a). The majority of these logs were reduced scale (1"=100') logs. A smaller area, of approximately 220 square miles in Milam, Burleson and Lee Counties was chosen for detailed investigation based on the availability of closely spaced well control and expanded scale (5"=100' and 2"=100'), detailed well logs (Fig. 5b). This detailed study area contains 215 logs, approximately 55% of the regional total, most of which are spontaneous potential/resistivity logs recorded on both 2 inch = 100 feet and 5 inch = 100 foot scales. Use of these logs permitted the delineation of genetic subunits within the Navarro 'A' and 'B' intervals. Correlations were also made with greater confidence and mapping of relatively thin units was possible.

In order to develop an understanding of the depositional systems and history of the Navarro 'A' and 'B' sandstones, the aforementioned subsurface data were utilized to construct 1) two regional and two detailed stratigraphic/lithologic cross-sections, 2) four regional and six detailed net-sandstone distribution maps, and 3) three regional interval isopachous maps. Cross-sections use the upper 'A' marker horizon as a datum unless otherwise noted (Figs. 3 and 4). This datum consists of a low-resistivity shale, immediately underlying the highly-resistive basal Midway glauconitic sand, which has a distinctive log character (Figs. 3 and 4) and is found throughout the study area. Gamma-ray logs also exhibit a sharp positive response at the base of this marker bed. Net-sandstone determinations were made from measurement of deflections on spontaneous-potential logs. Spontaneous potential deflection was used to infer relative mud content of the sandstone intervals according to the amplitude of their responses.

Because spontaneous potential response varies according to the chemistry of formation waters and commonly from one instrument to another, the determination of whether a particular deflection represents a 'clean sandstone' or 'shaley sandstone' must be judged on each log by comparison with deflections corresponding to known 'clean sandstone' responses on that log. This calibration was difficult in some logs, but most of the available logs contained inferred 'clean sandstone' intervals that consistently gave highly negative spontaneous potential readings. The net-sandstone maps presented in this paper are conservative in respect to the amount of sand portrayed. Spontaneous potential responses on logs may be subdued by loss of permeability due to secondary cementation or a variety of factors other than increasing shale content. Only strong spontaneous potential responses were used in constructing the maps.

Shales from a conventional core taken through the Navarro 'A' interval and one from the Navarro 'B' interval provided microfauna for paleobathymetric estimates of the depositional environments of these interbedded sandstones and shales (Fig. 5b). These microfaunal assemblages (Table 2) were compared with Tertiary assemblages of the same genera, which have known bathymetric ranges, and are used as paleobathymetric indicators (Bathymetric distribution of Cretaceous foraminifers are not fully understood). These comparisons suggest that both the Navarro 'A' and 'B' sandstones were deposited in a mid- to outer-shelf setting (H. Billman and L. Soar, personal communication).

NAVARRO 'B' INTERVAL

Table 2 - Microfossil Assemblages from Navarro 'A' and 'B' Intervals

TABLE 2

Microfossil Assemblages

Navarro 'A' Interval J.A. Leonard - Flentge #1	Navarro 'B' Interval Lambert Hollub - Richards #3
Ammobaculites texanus	Ammobaculites sp.
Anomalina pseudopapillosa	Anomalina pseudopapillosa
Bolivina sp.	Haplophragmoides excavatus
Globotruncana gansseri	Lenticulina (Robulus) navarroensis
Haplophragmoides excavatus	Lenticulina sp.
Haplophragmoides rugosus	Trochammina sp.
Haplophragmoides sp.	
Heterohelix sp.	
Lenticulina (Robulus) navarroensis	
Pulsiphonina prima	
Quinculoculina antiqua angusta	

See Figures 5a and 5b for Core Locations

The Navarro 'B' sandstone interval is the older and stratigraphically lower of the two Kemp Clay (Upper Navarro Clay) shelf sandstones within the regional study area (Figs. 3 and 5) and will be discussed first. Three regional net-sandstone thickness maps and two regional interval isopachous maps were constructed to delineate the sandstone distribution within the Navarro 'B' shelf system and to identify the major depositional axes. In addition, four detailed net-sandstone thickness maps, corresponding to the four subunits of the 'B' interval, were compiled from the dense well control within the detailed study area to document successive changes in the sand dispersal patterns.

Regional Net-sandstone Geometries - Navarro 'B' Interval

The regional distribution of the Navarro 'B' sandstones is illustrated in figure 7. Two areas of significant sandstone accumulation can be distinguished. The larger, southern-most depocenter attains a maximum net-sandstone thickness of 55 ft (17 m) approximately 4.5 miles (7.3 km) southeast of the town of Minerva and has, therefore, been designated the "Minerva depocenter" (Fig. 7). The smaller, northern depocenter, which has a maximum net-sandstone thickness of only 25 ft (7.6 m) and lies in the northern corner of Milam County. This accumulation will be referred to as the "North Milam 'B' depocenter" (Fig. 7). Since well control is concentrated in the vicinity of the Minerva depocenter, discussion of the Navarro 'B' deposits will concentrate on the sandstones developed in this area.

Trending southwest from the Minerva depocenter is a linear sandstone thickening that is suggestive of a strandplain/barrier system (Fisher, et al,

FIGURE 7. - Composite net sandstone map for the Navarro 'B' interval showing sandstone distribution and regional cross-section locations. Boundaries of detailed study area are indicated by crosses.

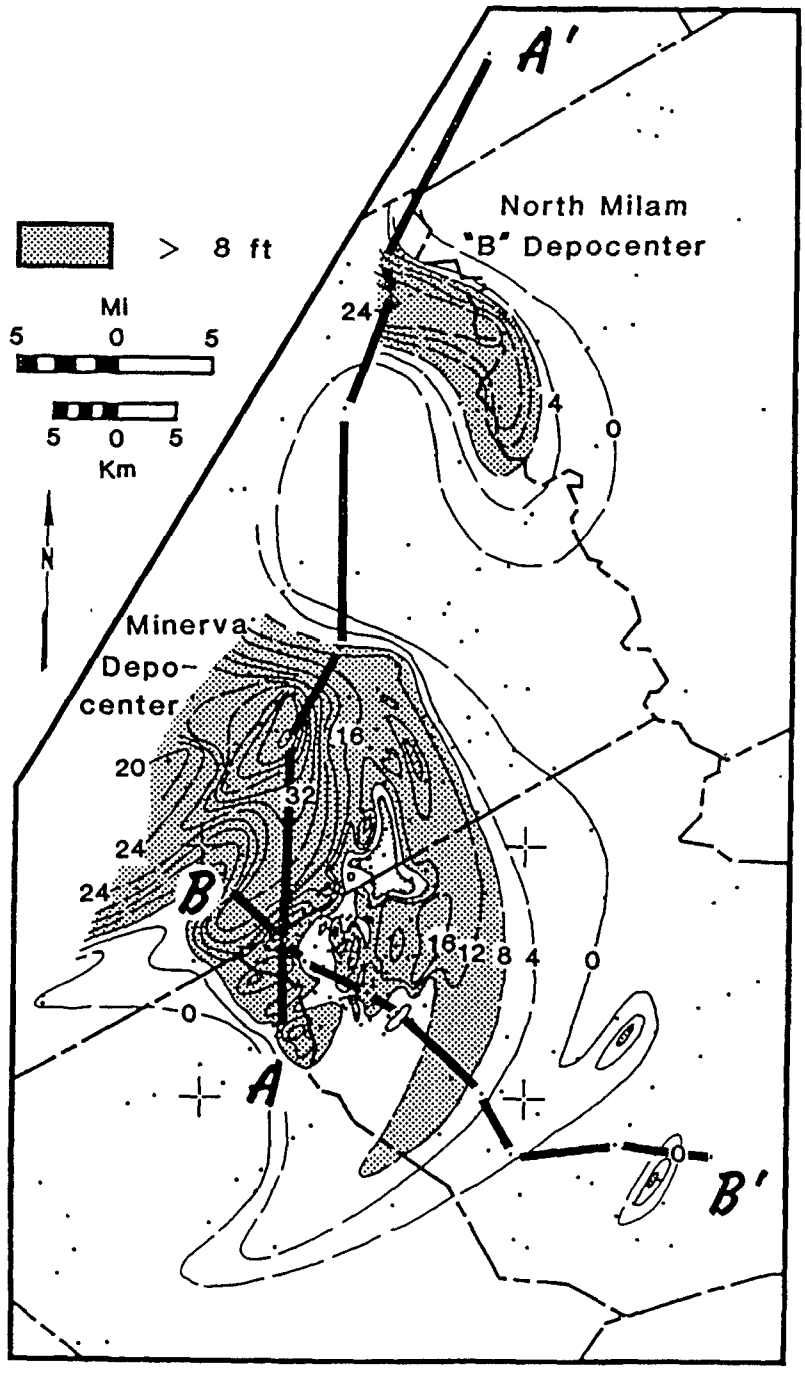
A'
North Milam
"B" Depocenter
> 8 ft
Mi
5 0 5
5 0 5
Km
N
Minerva
Depo-
center
24
4
0
20
16
32
24
24
B
0
16
12
8
4
0
0
A
0
B'

1969). Downdip from the Minerva depocenter, the Navarro 'B' sandstones extend 21 miles (34 km) into the basin and 27 miles (44 km) south-southwestward, along depositional strike, forming a 14-17 mile (22-28 km) wide arcuate belt of thin (3-15 ft; 1-4.6 m) marine sandstones (Fig. 7). This 'plume'-shaped distribution pattern is believed to be the result of reworking of delta-supplied sands by a south-southwesterly flowing coastal or shelf current under conditions similar to those described for the Nile River delta/Sinai shelf system by Coleman et al, (1981).

Hagar and Brown (1924) described sandstones in the Minerva-Rockdale oil field, located over the Minerva depocenter (Fig. 7), as ranging in thickness from 6-80 ft (2-24 m) using drillers' logs. These 'Minerva sands' were interbedded with shell beds and dark shales and lay 125-130 ft (38-40 m) below the top of the basal Midway glauconitic sandstone ('greensand') at a total depth of 640-650 ft (195-198 m). This glauconitic marker (Figs. 3 and 4) can be correlated basinward into the detailed study area using electric logs and verifies that the 'Minerva sands' are equivalent to the Navarro 'B' shelf sandstones and most probably comprise deltaic deposits associated with the Minerva depocenter. The North Milam 'B' depocenter also exhibits a thinner (5-25 ft; 1.5-7.6 m), plume-shaped distribution of shelf sandstones basinward and down-paleocurrent from the Minerva depocenter (Fig. 7).

The stratigraphic relationship of these two depocenters is illustrated in the regional strike section A-A' (Fig. 8a). The basinward thinning from 55 to 5 ft (17 to 1.5 m) of the Minerva depocenter sandstones is shown in the regional dip cross-section B-B' (Fig. 8b). This stratigraphic dip section

FIGURE 8. - **A.** Regional strike section A-A'. Note the stratigraphic and geometric relationships of the Navarro 'A' and 'B' deposits. **B.** Regional dip section B-B' illustrating basinward thinning of B1-3 and B-4 genetic units and basinward thickening of 'A' deposits. Cross-section locations shown in figure 7. Datum is Navarro 'A' marker shale.

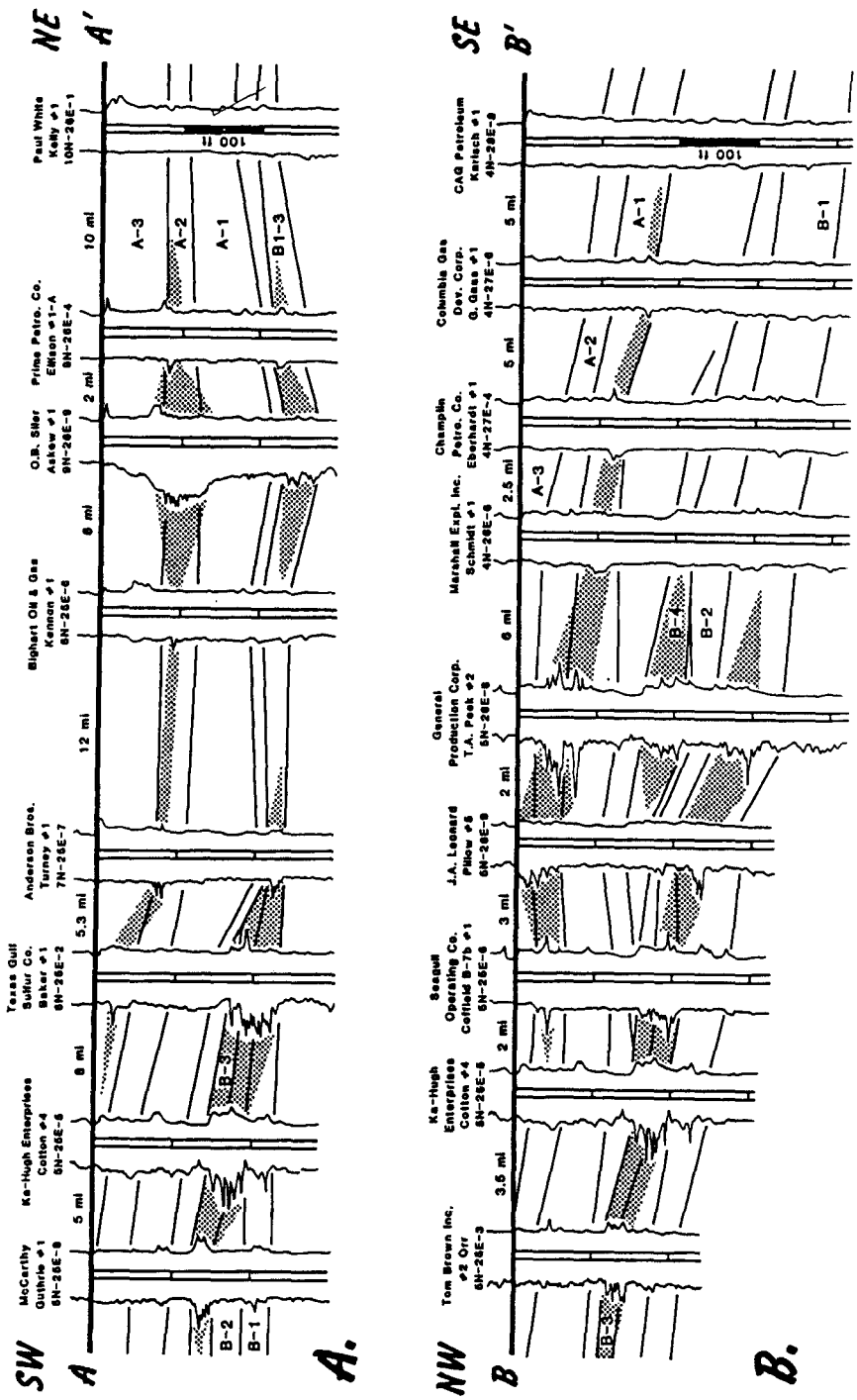
SW
A
NE
A'
McCarthy Guthrie #1 6N-26E-8
Ke-Hugh Enterprises Colton #4 6N-26E-6
Texas Gulf Sulfur Co. Baker #1 6N-26E-2
Anderson Bros. Turney #1 7N-26E-7
Bighart Oil & Gas Kennon #1 6N-26E-6
O.B. Siler Askew #1 6N-26E-8
Prime Petro. Co. Ellison #1-A 6N-26E-4
Paul White Kelly #1 10N-26E-1
5 mi
8 mi
5.3 mi
12 mi
8 mi
2 mi
10 mi
100 ft
A-3
A-2
A-1
B1-3
B-3
B-2
B-1
A.
NW
B
SE
B'
Tom Brown Inc. #2 Orr 6N-26E-3
Ke-Hugh Enterprises Colton #4 6N-26E-6
Seaqua Operating Co. Coltield B-7b #1 6N-26E-6
J.A. Leonard Pillow #6 6N-26E-8
General Production Corp. T.A. Peak #2 6N-26E-6
Marshall Expl. Inc. Schmidt #1 4N-26E-6
Champlin Petro. Co. Eberhardt #1 4N-27E-4
Columbia Gas Dev. Corp. G. Gase #1 4N-27E-6
CAG Petroleum Karlach #1 4N-26E-6
3.5 mi
2 mi
3 mi
2 mi
6 mi
2.5 mi
5 mi
5 mi
100 ft
A-3
A-2
A-1
B-4
B-2
B-1
B-3
B.

also reveals that the sandstones in the B-4 subunit are isolated from those of the B1-3 subunits by approximately 50 ft (15 m) of marine shale. This relationship can also be seen on the regional and detailed type electric logs (Figs. 3 and 4, respectively). For this reason, subunits B-1 through B-3 have been mapped as a single genetically-related depositional package in the regional area (Fig. 9a and b) while the B-4 subunit has been mapped separately (Figs. 9c and d). Two distinct shelf sandstone plume systems can be mapped in the Navarro 'B' interval (Figs. 9a and c). Due to the loss of interbedded marine shales near the Minerva depocenter, distinction of the B-4 sandstones from the B1-3 sandstone complex becomes increasingly difficult in this area. The dashed line at the landward end of the B-4 sand ribbon (Fig. 9c) indicates the area in which the distinction of the B-4 deposits from the B1-3 deposits becomes unreliable.

A notable feature of the B1-3 net-sandstone distribution map (Fig. 9a) is the presence of elongate intra-plume sandstone ridges. These ridges vary in thickness from 3 to 15 ft (1 to 5 m) and have average lengths of .75 to 6.5 mi (1.2 to 10.5 km), with widths of approximately .4 to 1.2 mi (.6 to 2 km). The orientation of their long axes varies, depending on their position relative to the Minerva depocenter. In the up-paleocurrent (proximal) area of the B1-3 plume system, ridge axes are dip-oriented and trend 23^{o}-45^{o} east of south. The trends of these linear features becomes more strike-oriented (50^{o}-55^{o} west of south) in the south-southwest or down-paleocurrent (distal) portions of the plume (Fig. 9a). This shift in orientation of shelf-bar axes with increasing distance down-current is believed to be due to a change in effective shelf current direction in the

FIGURE 9. - A. Composite regional net sandstone map of the B1-3 interval. Contour interval is 4 ft. Note linear trends within plume interior. **B.** Composite regional interval isopachous map of the B1-3 genetic unit. Contour interval is 20 ft. **C.** Regional net sandstone map of the B-4 subunit. Dashed line represents up-dip limit of subunit recognition. **D.** Regional interval isopachous map of the B-4 subunit. Note basinward shift of deposits relative to the B1-3 deposits (Fig. 9b). Contour interval is 20 ft.

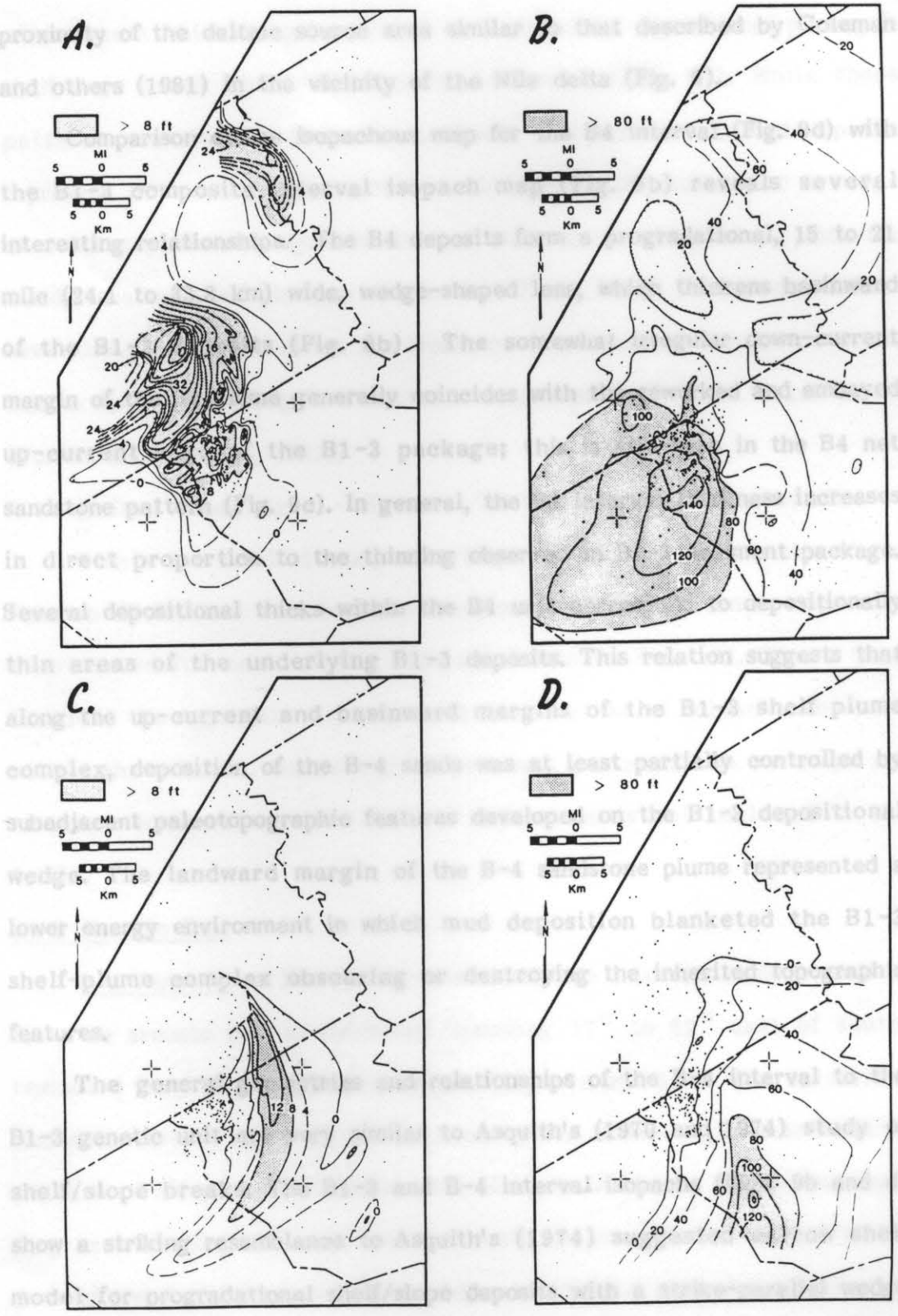
A.
> 8 ft
MI
5 0 5
5 0 5
Km
N
24
0
4
16
20
32
24
24
0
8
4
0
B.
> 80 ft
MI
5 0 5
5 0 5
Km
N
20
40
60
40
20
20
100
140
80
120
100
60
40
0
C.
> 8 ft
MI
5 0 5
5 0 5
Km
N
12
8
4
0
0
D.
> 80 ft
MI
5 0 5
5 0 5
Km
N
0
20
40
60
80
100
60
0
120
40
20
0

proximity of the deltaic source area similar to that described by Coleman and others (1981) in the vicinity of the Nile delta (Fig. 6).

Comparison of the isopachous map for the B4 interval (Fig. 9d) with the B1-3 composite interval isopach map (Fig. 9b) reveals several interesting relationships. The B4 deposits form a progradational, 15 to 21 mile (24.1 to 33.8 km) wide, wedge-shaped lens, which thickens basinward of the B1-3 deposits (Fig. 8b). The somewhat irregular down-current margin of the B4 plume generally coincides with the reworked and embayed up-current edge of the B1-3 package; this is also seen in the B4 net sandstone pattern (Fig. 9c). In general, the B4 interval thickness increases in direct proportion to the thinning observed in B1-3 sediment package. Several depositional thicks within the B4 unit correspond to depositionally thin areas of the underlying B1-3 deposits. This relation suggests that along the up-current and basinward margins of the B1-3 shelf plume complex, deposition of the B-4 sands was at least partially controlled by subadjacent paleotopographic features developed on the B1-3 depositional wedge. The landward margin of the B-4 sandstone plume represented a lower energy environment in which mud deposition blanketed the B1-3 shelf-plume complex obscuring or destroying the inherited topographic features.

The general geometries and relationships of the B-4 interval to the B1-3 genetic unit are very similar to Asquith's (1970 and 1974) study of shelf/slope breaks. The B1-3 and B-4 interval isopachs (Figs. 9b and d) show a striking resemblance to Asquith's (1974) suggested narrow shelf model for progradational shelf/slope deposits with a strike-parallel wedge

of sediment thickening basinward of the previous depositional package's shelf/slope break and then thinning basinward (Fig. 8b). While these patterns are similar, it is not believed that the B1-3 or B-4 deposits represent an actual progradational shelf/slope system, but rather a wedge of delta-supplied terrigenous clastics which accreted basinward onto the muddy, shallow shelf platform of the East Texas Basin. These conditions have also been described for the Woodbine (Cenomanian) current-reworked marine sandstones along the eastern margin of the East Texas basin (Turner and Congers, 1981).

Detailed Study Area - Navarro 'B' Net-sandstone Geometries

Within the detailed study area (Figs. 5a and b), the subunits of the Navarro 'B' interval were correlated and net sandstone thickness maps were constructed for each of the four subdivisions (Fig. 10). These maps illustrate the aggregate thickness and distribution of 'clean' sandstone within the subunit. Sandstone thicknesses portrayed on the maps are somewhat conservative since 'shaley' sandstone is not included in the totals.

B1-3 Genetic Unit

B-1 Subunit - The lower-most sandstone interval, designated B-1, forms an arcuate belt of sandstone trending 17° to 22° east of south, basinward from the Minerva depocenter (Figs. 9a and 10a). The up-current and down-current edges of this sandstone plume exhibit digitate or serrated patterns. This pattern coincides with elongate sandstone ridges that have long axes trending 12° to 25° west of south and are oriented oblique to the general trend of the plume. These ridges are 0.4-1.2 miles (.6-2 km) wide,

FIGURE 10. - A-D. Net sandstone maps of B1-4 subunits within detailed study area. Shift of sand deposition (Figs. 12a-d) to southwest reflects downcurrent reworking.

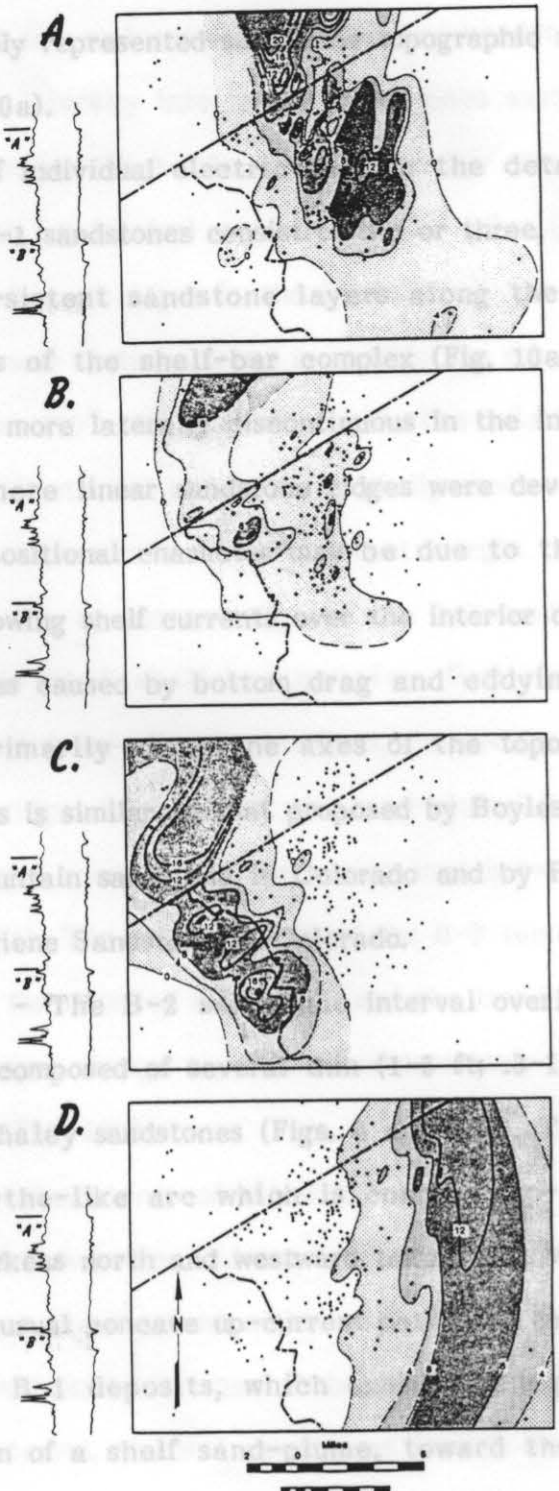
A.
B.
C.
D.
N
Miles
Kilometers

1.5-6.5 miles (2.5-10.5 km) long and have a maximum thickness of 3-15 ft (1-5 m) and probably represented submarine topographic relief of less than 10 ft (3 m) (Fig. 10a).

Comparison of individual electric logs in the detailed study area suggests that the B-1 sandstones consist of two or three, 5-10 ft (1.5-3 m) thick, laterally persistent sandstone layers along the up-current and basinward margins of the shelf-bar complex (Fig. 10a). This sheet-like character becomes more laterally discontinuous in the interior of the B-1 plume complex where linear sandstone ridges were developed (Fig. 10a). This change in depositional character may be due to the dissipation of energy of the winnowing shelf currents over the interior of the sand-plume. The lower velocities caused by bottom drag and eddying would tend to transport sand primarily along the axes of the topographically higher ridges. This process is similar to that proposed by Boyles and Scott (1982) for the Duffy Mountain sandstone in Colorado and by Porter and Weimer (1982) for the Hygiene Sandstone in Colorado.

B-2 Subunit - The B-2 sandstone interval overlies the B-1 sheet sandstones and is composed of several thin (1-5 ft; .3-1.5 m) interbedded sandstones and shaley sandstones (Figs. 4 and 10b). The B-2 sandstones form a broad scythe-like arc which is concave up-current, to the northeast, and thickens north and westward toward the Minerva depocenter (Fig. 10b). This unusual concave up-current pattern is the result of current reworking of the B-1 deposits, which exhibit the expected convex up-current distribution of a shelf sand-plume, toward the southwest as a migrating sand-wave front. The axis of this elongate lens has shifted

approximately 4.5 mi (7.5 km) to the southwest of the B-1 shelf sandstone-plume axis. The B-2 interval consists of a 'shaley' sandstone horizon which thickens and grades laterally into 'clean' sandstones southwest of the B-1 sandstone-plume complex (Figs. 10a and b). Locally, some B-2 sandstone ridges, .4-.75 miles (.6-1.2 km) wide by .75-2.3 miles (1.2-3.5 km) long, overlie ridges that formed ridges in the interior of the B-1 sandstone-plume. These B-2 linear features trend in roughly the same direction as the B-1 sandstone ridges (10^{o}-20^{o} west of south). The relationship of the two sets of ridges is illustrated in the detailed dip cross-section C-C' (Fig. 11a). This section transects the down-current margin of the B-1 sand-plume complex and the up-current edge of the B-2 sandstone belt. Within the interior of the B1-3 shelf-bar complex, B-2 ridges tend to be developed above, and down-paleocurrent from, the previously deposited B-1 ridges. Where B-2 ridges formed near the sand-plume margins, they are thinner and primarily occupy the intervening lows between B-1 sandstone thickenings (Fig. 11a). The net thickness of the B-2 sandstone increases in the western half of the detailed study area and the trend of the linear axes of the sandstone ridges change to a more southwesterly orientation, 52^{o} to 60^{o} west of south (Fig. 10b).

B-3 Subunit - Sandstones of the B-3 interval lie stratigraphically above the B-2 sandstone bodies and are laterally and vertically gradational with them. Sandstone development within the younger interval is confined primarily to the southwestern corner of the detailed study area (Fig. 10c). As with the B-2 interval, the B-3 sandstones form a 5-6 mile (8-10 km) wide, concave up-paleocurrent arcuate belt of sandstone. These deposits

FIGURE 11. - A. Detailed dip cross-section C-C' illustrating intra-plume sandstone distribution. Note development of ridges in plume interior. **B.** Detailed strike cross-section D-D' showing stratigraphic climbing of the B1-3 sandstones to the southwest. Note the stratigraphic isolation of the B-4 deposits from the B1-3 deposits. The Navarro 'A' sandstones also exhibit stratigraphic climbing to the southwest. Cross-section locations shown on figure 5b.

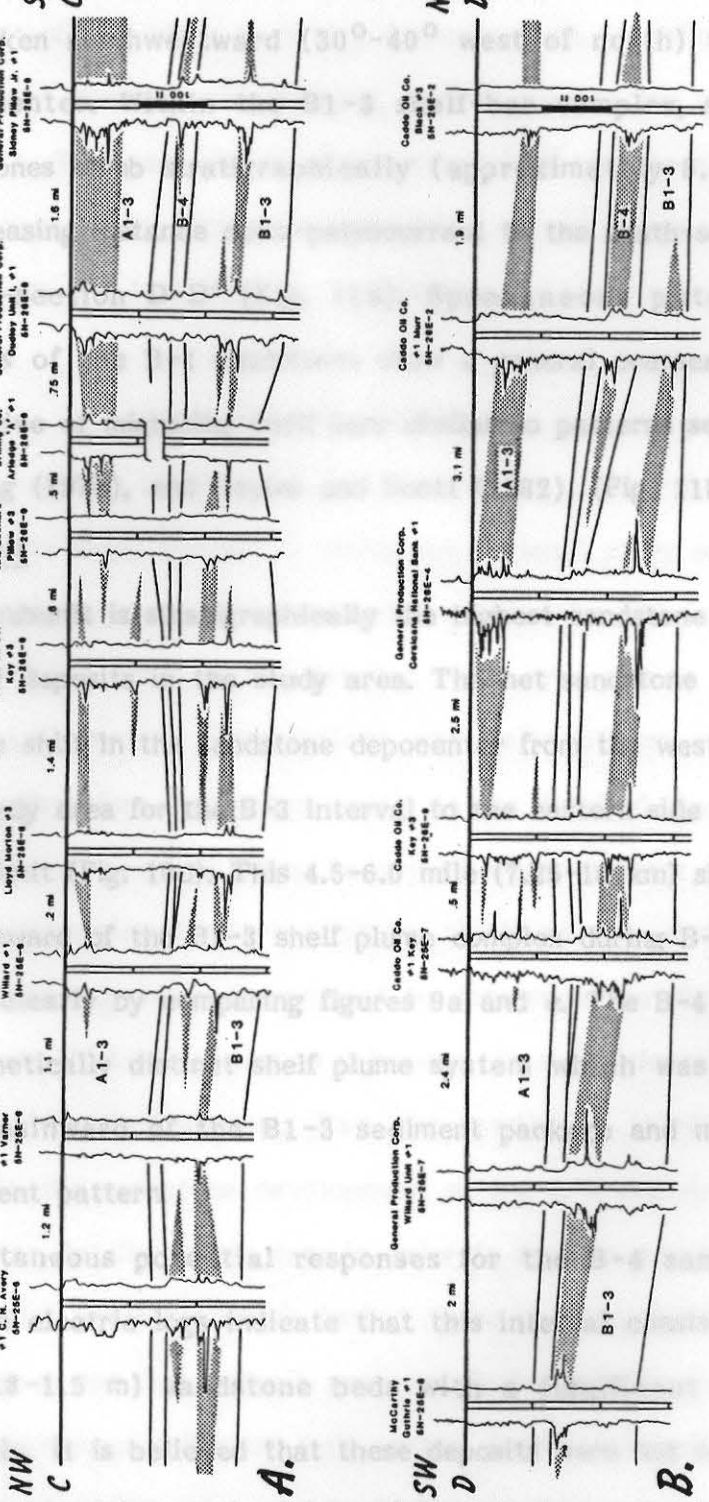
NW
C
A.
SE
C'
A1-3
B1-3
B-4
SW
D
B.
NE
D'
A1-3
B1-3
B-4

are concentrated in southwest trending (50^{o}-55^{o} west of south) linear ridges and thicken northwestward (30^{o}-40^{o} west of north) toward the Minerva depocenter. Within the B1-3 shelf-bar complex, successively younger sandstones climb stratigraphically (approximately 8.8 feet per mile) with increasing distance down-paleocurrent to the south-southwest as seen on cross-section D-D' (Fig. 11b). Spontaneous potential log characteristics of the B-3 sandstones show a general coarsening upward pattern suggestive of migrating shelf bars similar to patterns seen by Berg (1975), Spearing (1976), and Boyles and Scott (1982), (Fig. 11b).

B-4 Genetic Unit

The B-4 subunit is stratigraphically the highest sandstone interval of the Navarro 'B' deposits in the study area. The net sandstone map of this interval shows a shift in the sandstone depocenter from the western side of the detailed study area for the B-3 interval to the eastern side of the area for the B-4 subunit (Fig. 10d). This 4.5-6.0 mile (7.25-10 km) shift in sand deposition basinward of the B1-3 shelf plume complex during B-4 time can be seen more clearly by comparing figures 9a and c. The B-4 sandstones represent a genetically distinct shelf plume system which was deposited immediately basinward of the B1-3 sediment package and mimics their convex up-current pattern.

The spontaneous potential responses for the B-4 sandstones on expanded 5 inch electric logs indicate that this interval consists of many thin (1-5 ft; .3-1.5 m) sandstone beds with a significant amount of interbedded shale. It is believed that these deposits were not subjected to as much current winnowing as the 'cleaner' B-1 sandstone sheets and bars.

The narrow (4.5-9 miles; 7.25-14.5 km) B-4 sandstone ribbon exhibits much less development of secondary reworking features, such as oblique current-parallel ridges and stratigraphic climbing, than is seen in the more mature B1-3 shelf plume. This contrast in plume morphology may be attributed to a more rapid rate of deposition into somewhat deeper water, resulting in lower wave energy and less time for reworking.

NAVARRO 'A' INTERVAL

The Navarro 'A' interval is the uppermost zone of sandstone development in the Kemp Formation within the regional study area (Figs. 3 and 5). consistent recognition of subunits within the 'A' interval was difficult beyond the limits of the detailed study area due to the lack of closely spaced well control. Correlations and delineations of the A1-3 subdivisions was therefore confined primarily to the detailed study area and to the regional cross-sections (Figs. 8a and b) where greater well control was available. A regional net-sandstone thickness map and a regional interval isopachous map were constructed to determine the distribution of the entire Navarro 'A' interval and to delineate the major depositional axes of the Navarro 'A' shelf system. Two net-sandstone thickness maps, corresponding to the sandstone development of the A-2 and A-3 subunits, were made for the detailed study area in order to develop an understanding of the depositional processes which formed these shelf sandstone deposits. Thick sandstones of the A-1 subunit were not found within the detailed study area and lack of sufficient well control in the regional study area prevented the construction of a net-sandstone map for this subunit.

Regional Net-sandstone Geometries - Navarro 'A' Interval

Sandstone distribution within the Navarro 'A' interval is much more regional in extent than that of the Navarro 'B' interval. Figure 12a is a regional net-sandstone thickness map for the 'A' interval. A prominent depocenter with a maximum of 60 ft (18 m) of sandstone developed during 'A' deposition in the extreme northern part of the regional study area and is herein referred to as the North Milam 'A' depocenter. This designation will be used to differentiate these deposits from those of the Navarro 'B' from the same geographic area previously denoted as the North Milam 'B' depocenter (Figs. 7 and 9). The North Milam 'A' depocenter, is laterally somewhat less extensive than the Navarro 'B' deposits of the Minerva depocenter and exhibits a blocky spontaneous potential character (Fig. 8a) along its northern margin. Basinward of the depocenter, the net-sandstone contours are skewed to the south-southwest in a rather broad, arcuate ribbon similar to the pattern seen in the 'B' interval. It is also evident that the 'A' sandstones were depositionally detached from the shoreline in the vicinity of the Minerva ('B') depocenter and that they extended much farther basinward than the underlying 'B' sandstone deposits (Fig. 8b). Since no shoreline deposits were recognized in the regional study area and the North Milam 'A' depocenter is the only evidence of shoreline proximity, it must be assumed that the coastline, during Navarro 'A' deposition, lay to the west of the present Kemp outcrop, probably at a distance not much greater than 2-5 miles (3-8.0 km). The maximum basinward extent of 'A' sand deposition is encountered southeast of the detailed study area at a point approximately 40 miles (64 km) down dip from the Kemp outcrop.

FIGURE 12. - **A.** Composite regional net sandstone map of A1-3 interval. Note deflection of net sandstone trend in vicinity of underlying Minerva ('B') Depocenter and depositional platform. Contour interval is 4 ft. **B.** Regional isopachous map of Navarro A1-3 interval. Comparison with figures 11b and d suggests a basinward shift in deposition with respect to the Navarro B1-4 deposits. Contour interval is 20 ft.

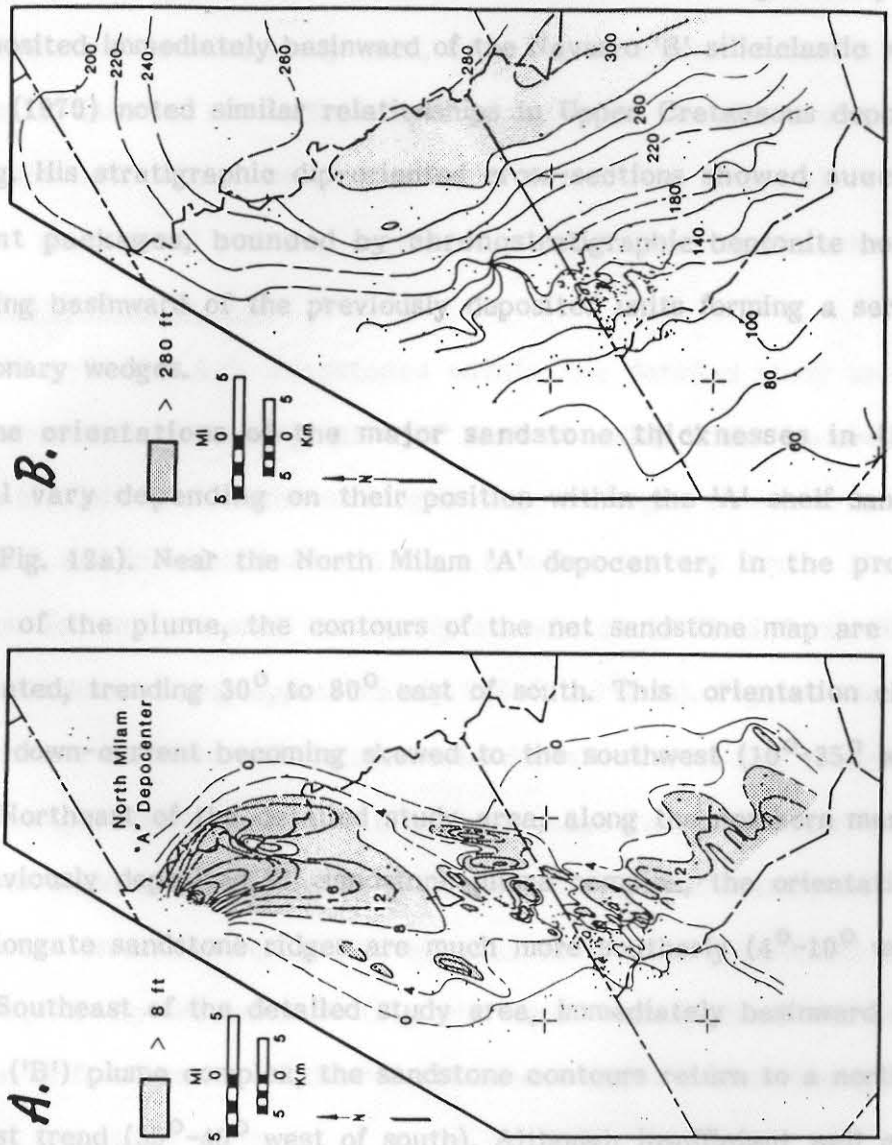
B.
> 280 ft
200
220
240
260
280
300
260
220
180
140
100
80
60
Mi
Km
A.
> 8 ft
North Milam
'A' Depocenter
16
12
8
4
0
Mi
Km

Net thickness of the Navarro 'A' interval is depicted in figure 12b. Comparison of this 'A' interval thickness map with those of the Navarro B1-3 and B-4 intervals (Figs. 9b and d, respectively) and the regional cross-section B-B' (Fig. 8b) reveals that the Navarro 'A' genetic package was deposited immediately basinward of the Navarro 'B' siliciclastic wedges. Asquith (1970) noted similar relationships in Upper Cretaceous deposits in Wyoming. His stratigraphic dip-oriented cross-sections showed successive sediment packages, bounded by chronostratigraphic bentonite horizons, thickening basinward of the previously deposited units forming a series of accretionary wedges.

The orientations of the major sandstone thicknesses in the 'A' interval vary depending on their position within the 'A' shelf sandstone plume (Fig. 12a). Near the North Milam 'A' depocenter, in the proximal portion of the plume, the contours of the net sandstone map are rather dip-oriented, trending 30^{o} to 80^{o} east of south. This orientation changes further down-current becoming skewed to the southwest (10^{o}-35^{o} west of south). Northeast of the detailed study area, along the northern margin of the previously deposited 'B' sandstone plume complex, the orientations of these elongate sandstone ridges are much more southerly (4^{o}-10^{o} west of south). Southeast of the detailed study area, immediately basinward of the Minerva ('B') plume complex, the sandstone contours return to a northeast-southwest trend (35^{o}-43^{o} west of south). Although insufficient well control was available to determine the net-sandstone contour trends in the region east of the detailed study area, it is believed that they would exhibit an intermediate value, or one slightly more northwest-southeast oriented, with

respect to the values north and south of this area. In the detailed study area, the long axes of the shelf-bars show a definite northeast-southwest orientation, trending 28^{o} to 35^{o} west of south.

Detailed Study Area - Navarro 'A' Net-sandstone Geometries

Within the detailed study area, only the upper two subunits of the Navarro 'A' interval are sufficiently distinct to be correlated and mapped with confidence. These two subunits, A-2 and A-3 (Fig. 4), are also somewhat gradational and may represent a depositional continuum.

A-2 and A-3 Genetic Unit

The A-2 and A-3 sandstones within the detailed study area form northeast-southwest trending (15^{o}-35^{o} west of south) linear features (Figs. 13a and b). Individual sandstone ridges range in length from 2 to 2.5 miles (3-4.0 km) and in width from 0.5 to 1.0 miles (.8-1.6 km). Maximum thickness for any one shelf bar rarely exceeds 10-15 ft (3-5 m) with the average thickness being approximately 2-6 ft (.6-2 m). Figures 13a and b demonstrate a landward shift in sandstone deposition from A-2 to A-3 time. Careful comparison of these net sandstone maps indicates that the 'A' sandstones climb stratigraphically both onshore (northwestward), and down-paleocurrent (southwestward). This conclusion is also supported by the stratigraphic dip section B-B' (Fig. 8b) which clearly shows this onshore and down-drift migration of the 'A' sandstones and the time-transgressive nature of successive units.

Correlation of closely spaced well logs suggests that the sandstone ridges , within the detailed study area, represented an accumulation of several (2-7) thin (1-10 ft; .3-3.0 m), imbricated, landward-accreting

FIGURE 13. - A-B. Net sandstone maps of A-2 and A-3 subunits within the detailed study area. Note onshore and down-current shift in sandstone distribution.

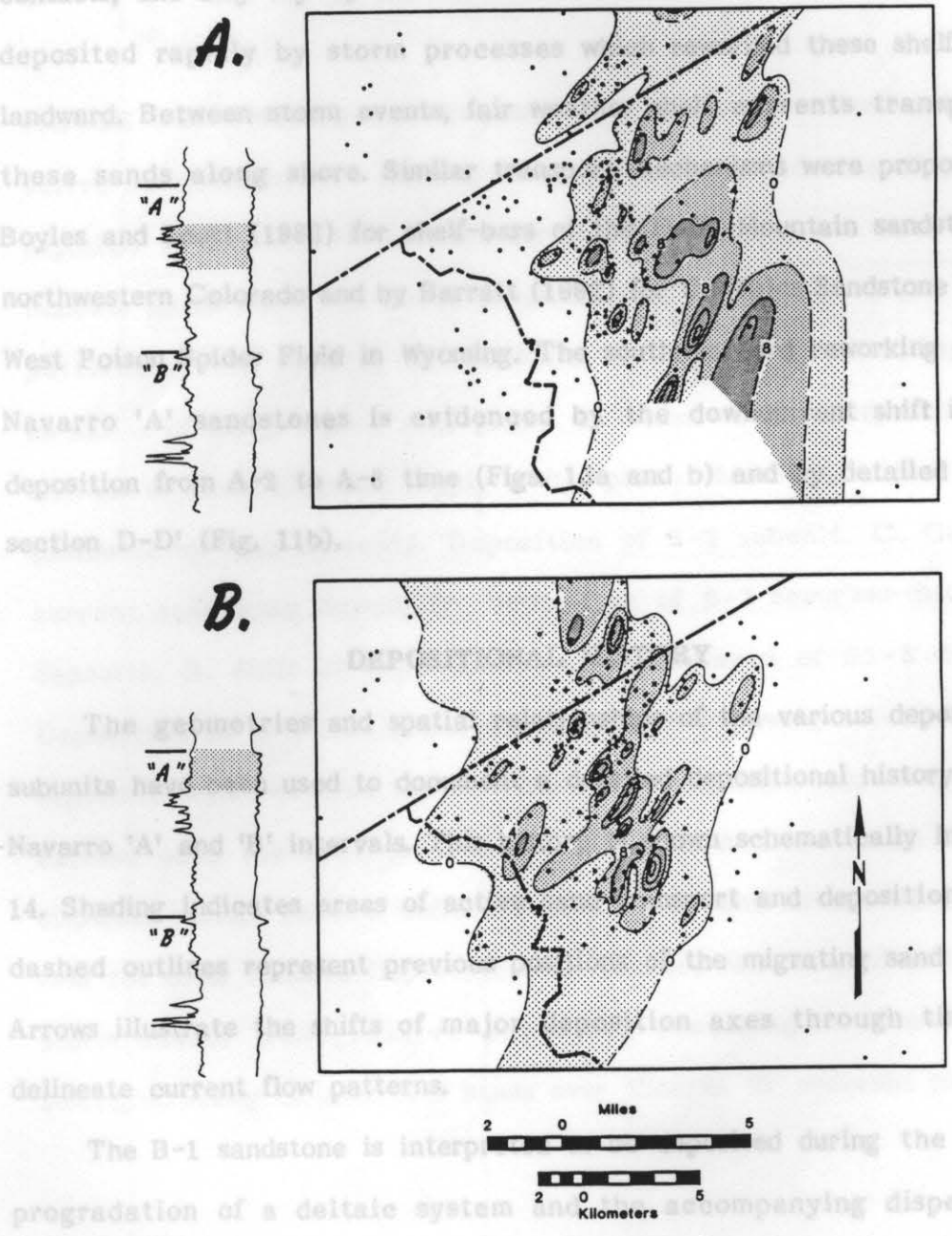
A.
"A"
"B"
B.
"A"
"B"
N
Miles
2 0 5
2 0 5
Kilometers

sandstone bodies. Primary sedimentary features in cores from these sandstones include soft sediment deformation structures, gradational upper contacts, and clay rip-up clasts. Individual thin sandstone beds were deposited rapidly by storm processes which reworked these shelf sands landward. Between storm events, fair weather shelf currents transported these sands along shore. Similar transport mechanisms were proposed by Boyles and Scott (1982) for shelf-bars of the Duffy Mountain sandstone of northwestern Colorado and by Barratt (1982) for the Fales Sandstone of the West Poison Spider Field in Wyoming. The southwestward reworking of the Navarro 'A' sandstones is evidenced by the downcurrent shift in sand deposition from A-2 to A-3 time (Figs. 13a and b) and by detailed strike section D-D' (Fig. 11b).

DEPOSITIONAL HISTORY

The geometries and spatial relationships of the various depositional subunits have been used to document a detailed depositional history of the Navarro 'A' and 'B' intervals. This history is shown schematically in figure 14. Shading indicates areas of active sand transport and deposition while dashed outlines represent previous positions of the migrating sand bodies. Arrows illustrate the shifts of major deposition axes through time and delineate current flow patterns.

The B-1 sandstone is interpreted to be deposited during the initial progradation of a deltaic system and the accompanying dispersal of sediments onto the shelf (Fig. 14a). In this early phase, the sand distribution pattern exhibits a high degree of dip orientation as axial jet

FIGURE 14. - Schematic Depositional History - Shading indicates active sedimentation. Dashed lines indicate boundaries of previous deposits. Arrows with "c" indicate current flow patterns and those with "p" indicate plume axes. **A.** Initial progradation and development of current patterns in the vicinity of the Minerva Depocenter resulting in the formation of the B-1 shelf sand-plume. **B.** Onshore shift of depositional axis and loss of direct sediment supply to B-1 plume. Reworking of B-1 sands to southwest by shelf currents. Deposition of B-2 subunit. **C.** Continued current reworking downdrift. Deposition of B-3 reworked distal plume deposits. **D.** Shift of depositional axis basinward of B1-3 complex. Deposition of B-4 sand-plume deposits. **E-G.** Following a period of shale deposition which covered the B1-4 shelf deposits, delta-supplied sands were carried onto the shelf from the North Milam 'A' Depocenter. A1-2 sand dispersal pattern reflects deflection of shelf currents around B1-4 platform near the older Minerva Depocenter. **H.** Onshore reworking of A-2 sands by storm and/or transgressive processes resulting in deposition of stratigraphically isolated A-3 sands over Minerva 'B' sediment platform.

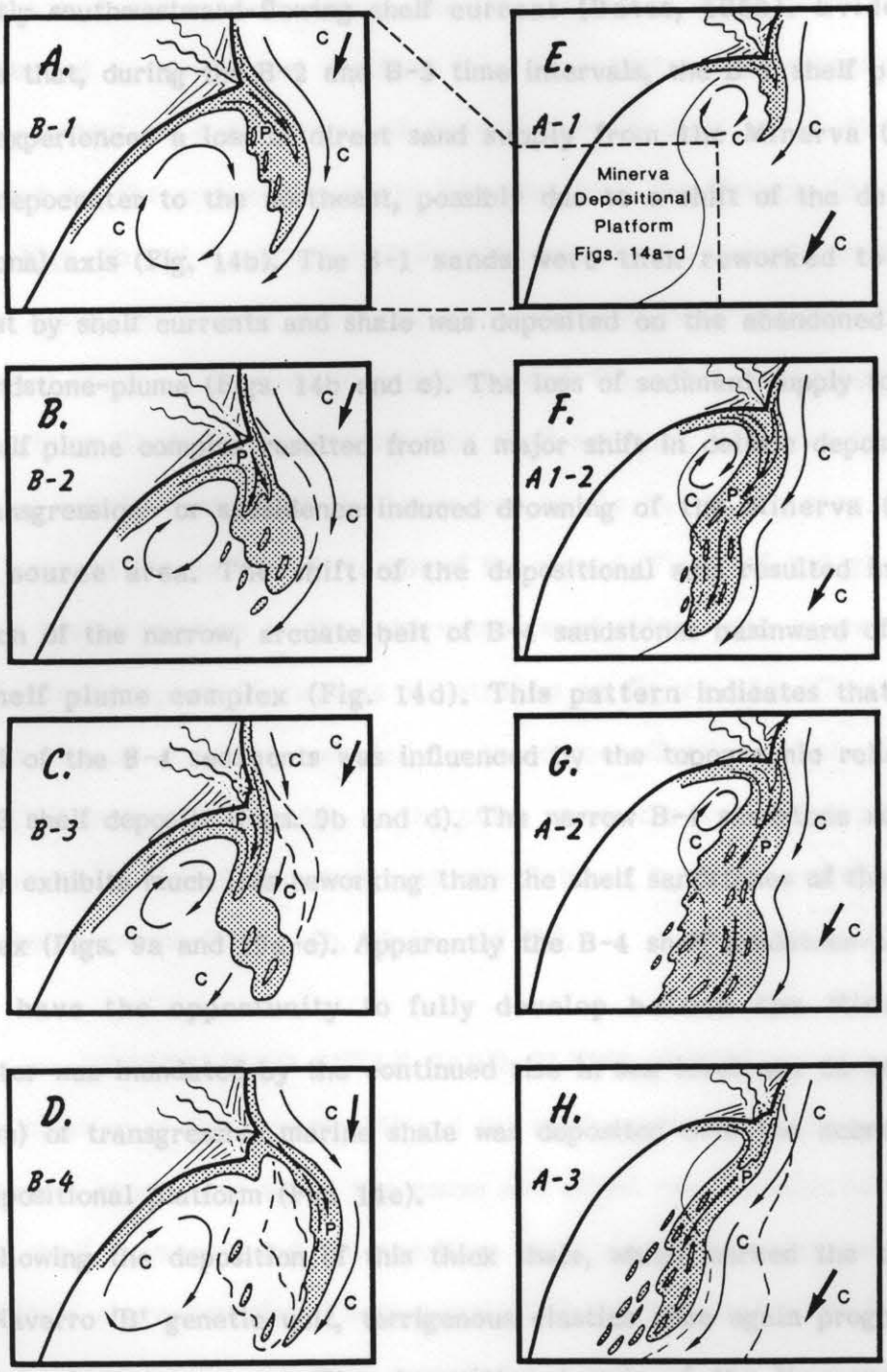
A.
B-1
E.
A-1
Minerva
Depositional
Platform
Figs. 14a-d
B.
B-2
F.
A1-2
C.
B-3
G.
A-2
D.
B-4
H.
A-3
C
P

flow injects sediment into the marine environment at a high angle to the dominantly southwestward-flowing shelf current (Bates, 1953). Evidence indicates that, during the B-2 and B-3 time intervals, the B-1 shelf plume system experienced a loss of direct sand supply from the Minerva ('B') deltaic depocenter to the northeast, possibly due to a shift of the deltaic depositional axis (Fig. 14b). The B-1 sands were then reworked to the southwest by shelf currents and shale was deposited on the abandoned B-1 shelf sandstone-plume (Figs. 14b and c). The loss of sediment supply to the B1-3 shelf plume complex resulted from a major shift in deltaic deposition or a transgression- or subsidence-induced drowning of the Minerva ('B') deltaic source area. The shift of the depositional axis resulted in the deposition of the narrow, arcuate belt of B-4 sandstones basinward of the B1-3 shelf plume complex (Fig. 14d). This pattern indicates that the dispersal of the B-4 sediments was influenced by the topographic relief of the B1-3 shelf deposits (Figs. 9b and d). The narrow B-4 sandstone ribbon (Fig. 9c) exhibits much less reworking than the shelf sandstones of the B1-3 complex (Figs. 9a and 10a-c). Apparently the B-4 shelf sandstone-plume did not have the opportunity to fully develop before the Minerva depocenter was inundated by the continued rise in sea level and 50-100 ft (15-30 m) of transgressive marine shale was deposited over the accreting B1-4 depositional platform (Fig. 14e).

Following the deposition of this thick shale, which marked the close of the Navarro 'B' genetic unit, terrigenous clastics once again prograded into the marine environment. The depositional axis of the Navarro 'A' deltaic/shelf system is located in northern Milam County in the same area

as the North Milam depocenter of the Navarro 'B' interval. Deposition of terrigenous mud and sand in advance of the prograding North Milam ('A') delta created a depositional platform (Fig. 14e) that accreted basinward and down-current as a sequence of sedimentary wedges which molded themselves to the paleotopography inherited from the Navarro 'B' shelf deposits (Figs. 9b and d, and 12b). Sediments, entrained by coastal currents near the delta and carried shelfward, were reworked down-current toward the detailed study area where they encountered the relict topography of the underlying B1-4 plume complex. The shelf currents, deflected by this obstructing relief, transported the lower and middle 'A' sandstones (A-1 and A-2) around the basinward margin of the mound (Figs. 14f and g). The change in the orientation of the intra-plume sand ridges with respect to this paleotopographic feature is illustrated in figure 12a. Continued deposition of sand and mud eventually reduced the effective relief of the Minerva ('B') sedimentary wedge to the point where the A-2 and A-3 shelf sands could be reworked landward, over the platform, by storm activity and fair weather currents (Figs. 14h, 13a-b and 8b).

GENERALIZED SHELF SAND-PLUME MODEL

Examination of the Navarro 'A' and 'B' shelf sandstone-plume systems yields several conclusions about the cause and effect relationships between inferred shelf processes and the resultant sandstone distribution patterns and lithologic characteristics. These conclusions are summarized in figure 15 using a 'general case' model for a mud-rich, current-swept shelf system. Some of the more significant trends which may be useful when incorporated

FIGURE 15. Shelf sand-plume morphology. An increasing thickness of plume-associated mudstones in the distal portion of the plume forms a muddy depositional platform over which the shelf sand bodies migrate. This pattern is exhibited in Figures 9a and b. Within the plume sand is concentrated near the depocenter and decreases in thickness downcurrent while stratigraphic isolation increases downdrift.

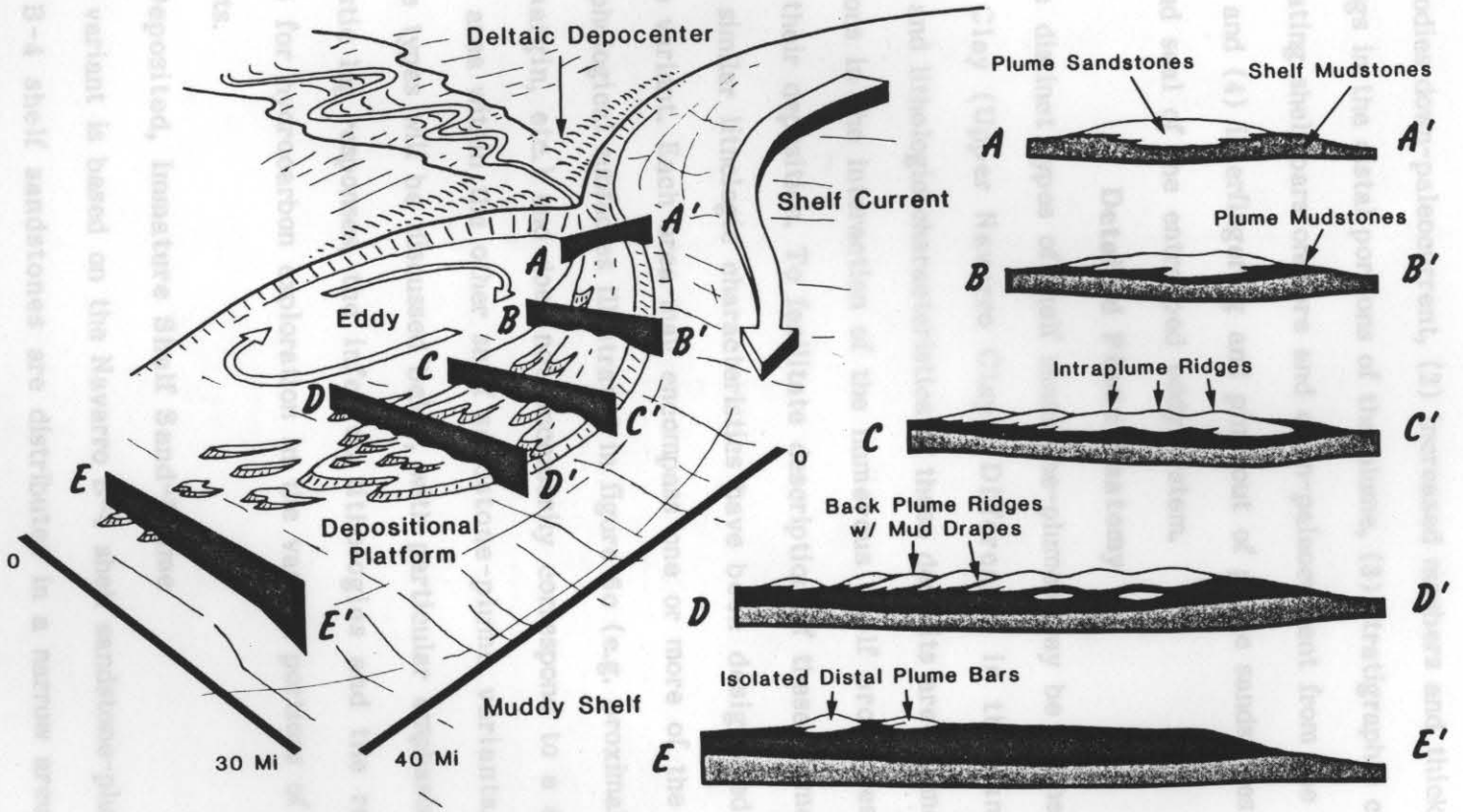
Deltaic Depocenter
Shelf Current
Eddy
A
A'
B
B'
C
C'
D
D'
E
E'
Depositional Platform
Muddy Shelf
0
30 Mi
40 Mi
Plume Sandstones
Shelf Mudstones
Plume Mudstones
Intraplume Ridges
Back Plume Ridges w/ Mud Drapes
Isolated Distal Plume Bars

into an exploration model include (1) increased stratigraphic isolation of sandstone bodies down-paleocurrent, (2) increased numbers and thickness of shale partings in the distal portions of the plume, (3) stratigraphic climbing of the migrating shelf-bars onshore and down-paleocurrent from the deltaic depocenter and (4) interfingering and pinchout of plume sandstones up-dip into the mud seal of the entrapped eddy system.

Detailed Plume Anatomy

Three distinct types of shelf sandstone-plumes may be delineated in the Kemp Clay (Upper Navarro Clay). Differences in the sandstone geometries and lithologic characteristics of these deposits are a function of the variations in the interaction of the numerous shelf processes which controlled their deposition. To facilitate description of these plume types, areas with similar lithologic characteristics have been designated within each plume variant. Each area may encompass one or more of the various plume morphological subfacies illustrated in figure 6c (e.g. proximal plume, seaward margin, etc.) and does not necessarily correspond to a similarly designated area within the other shelf sandstone-plume variants. These sand-plume types will be discussed below, with particular emphasis on the characteristic log responses, the inferred lithologies and the resulting potentials for hydrocarbon exploration in the various portions of each of the variants.

Rapidly Deposited, Immature Shelf Sand-Plume

This variant is based on the Navarro B-4 shelf sandstone-plume (Fig. 9c). The B-4 shelf sandstones are distributed in a narrow arcuate belt around the basinward margins of the B1-3 shelf sandstone complex (Fig. 16a).

FIGURE 16. - Rapidly deposited, immature shelf sandstone-plume - A. B-4 net sandstone map showing example electric log locations. Well Names - 1. O. B. Siler, Askew #1, 5N-25E-8; 2. C. L. Williams, Patzke #1, 8N-26E-1; 3. Caddo Oil, Co., Southwest Land #1, 6N-26E-1; 4. Hill International Prod. Co., Baron #1, 4N-26E-7; 5. Anderson Bros. Corp, Sallie Miller #1, 6N-25E-2; 6. J. A. Leonard, Smith, Coffield "B", 5N-26E-4. **B.** Selected electric log patterns. **C.** Schematic plume evolution. **D.** Inferred hydrocarbon potential. Poor = 1; Excellent = 5.

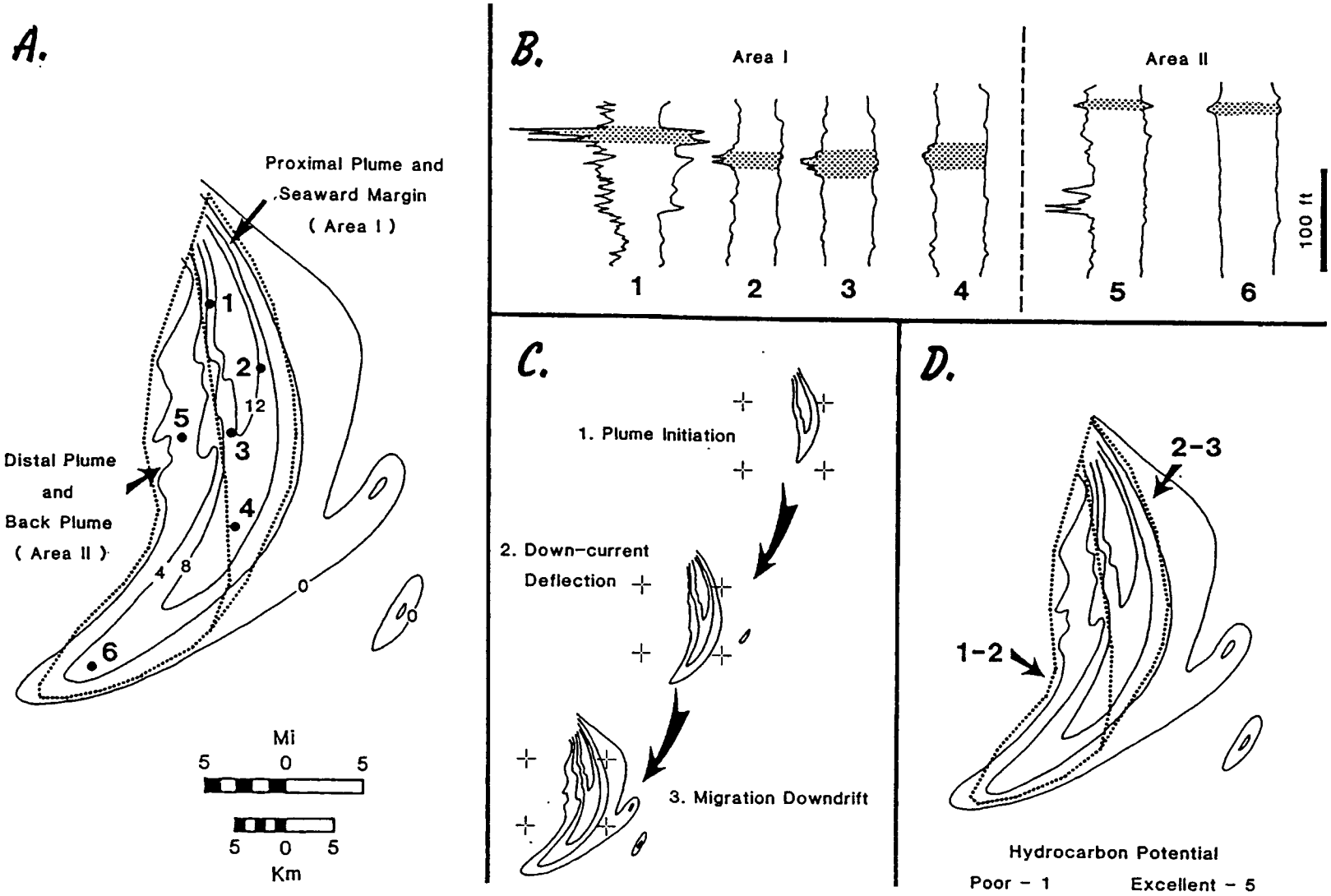
A.
Proximal Plume and
Seaward Margin
(Area I)
Distal Plume
and
Back Plume
(Area II)
1
2
12
3
4
5
6
4
8
0
0
Mi
5 0 5
5 0 5
Km
B.
Area I
Area II
1
2
3
4
5
6
100 ft
C.
1. Plume Initiation
2. Down-current
Deflection
3. Migration Downdrift
D.
2-3
1-2
Hydrocarbon Potential
Poor - 1
Excellent - 5

Proximal Plume and Seaward Margin (Area-1)- The thickest sandstones occur in the proximal and seaward portions of the plume axis. These deposits have a log response indicating relatively 'clean' sandstone with little associated shale (Fig. 16a-b). The proximity to the deltaic source and the up-current position in the plume contributed to the well-winnowed character of these sandstones. Despite the 'clean' nature of these deposits, the production potential remains somewhat marginal since hydrocarbons, unless impeded by local faulting, would tend to migrate up-dip to the deltaic Minerva depocenter.

Distal Plume and Back Plume (Area-2)- Electric log responses indicate that the sandstones within this area are extremely thin (1-5 ft; .3-1.5 m) with many shale breaks (Fig. 16b). The mud-rich nature of these deposits is interpreted as being the result of inadequate syndepositional winnowing by shelf currents. The rapid influx of the terrigenous material, probably associated with a deltaic avulsion (Fig. 14), provided insufficient time for these sediments to be reworked and sorted prior to termination of sand deposition caused by another delta lobe shift and/or a major marine transgression.

The thin, muddy nature of the sandstones and the large number of interbedded shale beds reduces the quality and areal extent of hydrocarbon reservoirs in the more distal areas of this type of shelf sandstone-plume. The exploration potential for rapidly deposited, immature sandstone-plumes is therefore rated as poor to fair.

Current-Reworked, Abandoned Shelf Sand-Plume

The dense well control in the vicinity of the Minerva depocenter, and

the adjacent B1-3 shelf plume complex, permitted the development of a detailed model for this delta-associated shelf sandstone-plume system. Figure 17a illustrates the spatial and geometric relationships of the Minerva deltaic depocenter to the B1-3 shelf sandstones. This deltaic/shelf complex can be subdivided into five areas which display unique electric log characteristics (Fig. 17b).

Depocenter (Area-1) - These sandstones correspond to the deltaic and delta front sandstones of the Minerva depocenter (Area-1, Fig. 17a). This sequence of stacked sandstones is bounded up-dip by marine and non-marine shales and has been a prolific hydrocarbon producing horizon since its initial discovery in 1921 (Hagar and Brown, 1924; Texas Railroad Commission-1982 Petroleum Production Figures).

Proximal Plume and Seaward Margin (Area-2) - The proximal sandstones of this zone represent the initial progradation of these sands into the shelf environment and corresponds to the Navarro B-1 interval. The intense winnowing, by shelf currents, of the proximal portion and seaward margin of the shelf sand plume resulted in the deposition of relatively thick, laterally persistent, sheet-like deposits of 'clean' sand in this area (Fig. 17). Trapping of hydrocarbons in these sandstones is primarily associated with faulting which impeded fluid migration up-dip into the sandstones of the Minerva depocenter (Area-1).

Mid-Plume (Area-3)- This is the area through which the current-reworked B-1 sands migrated after the supply of sand from the Minerva depocenter was halted by a landward shift in the depositional axis. Abandonment of the B-1 'plume' resulted in the down-current migration of

FIGURE 17. - Current-reworked, abandoned shelf sandstone-plume - A. B1-3 net sandstone map showing example electric log locations. Well Names - 1. Texas Gulf Sulfur Co., Baker #1, 6N-25E-2; 2. Mustang Petrol. Co., Calloway #1, 6N-25E-1; 3. J. A. Leonard, Flentge #1, 5N-26E-4; 4. Seagull Oper. Co., Coffield B7b - #1, 5N-25E-6; 5. McCarthy, Guthrie #1, 5N-26E-8; 6. Tom Brown, #2 Orr, Inc., 5N-25E-3. **B.** Selected electric log patterns. **C.** Schematic plume evolution. **D.** Inferred hydrocarbon potential. Poor = 1; Excellent = 5.

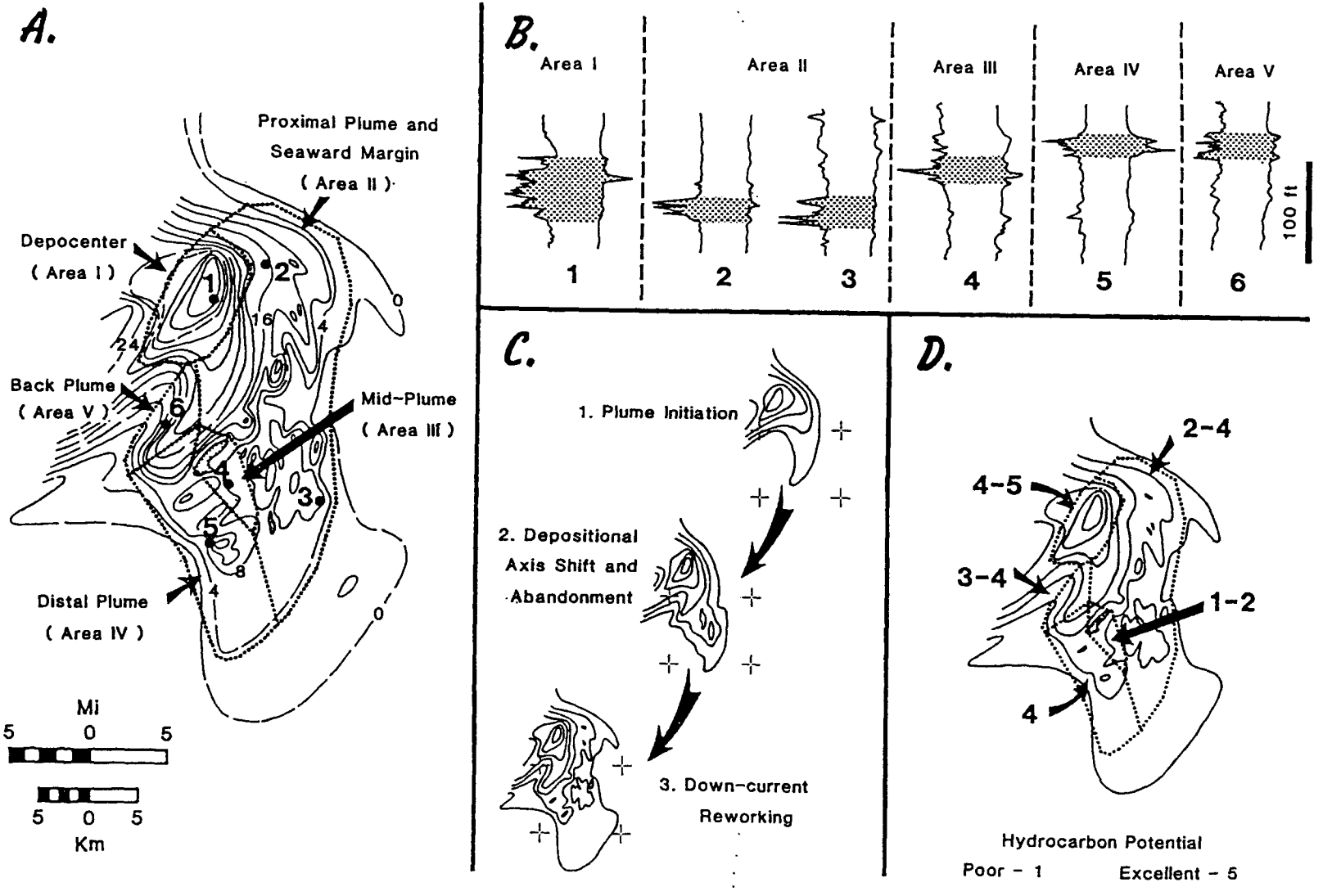
A.
Proximal Plume and
Seaward Margin
(Area II)
Depocenter
(Area I)
Back Plume
(Area V)
Mid-Plume
(Area III)
Distal Plume
(Area IV)
Mi
5 0 5
5 0 5
Km
B.
Area I
Area II
Area III
Area IV
Area V
100 ft
1
2
3
4
5
6
C.
1. Plume Initiation
2. Depositional
Axis Shift and
Abandonment
3. Down-current
Reworking
D.
2-4
4-5
3-4
1-2
4
Hydrocarbon Potential
Poor - 1
Excellent - 5

a transverse belt of linear sand ridges (Figs. 10a-c and 14a-c). Because there was little or no sand influx from the deltaic source, movement of the sand bodies through this area was transient and left only a blanket of muddy sand with a few isolated sand ridges; the majority of sand migrated on down current into the distal portion of the plume (Fig. 17 a-b). The poor sand quality and large number of shale partings in this an area gives it marginal to poor hydrocarbon exploration potential.

Distal Plume (Area-4)- This area represents the maximum extent of down-current migration of the reworked B-1 sands. This area corresponds to the B-3 and part of the B-2 sandstone intervals and exhibits thick (10-25 ft; 3-7.5 m) well-developed sandstone bodies which pinch-out rapidly down-current and grade laterally up-current into the highly-imbricated and poorly developed sandstone stringers of the mid-plume (Fig. 11b and 17a). The shale-encased nature of these stacked sandstone bodies, often in combination with tectonic faulting, accounts for the high hydrocarbon potential for this portion of the Navarro 'B' shelf sandstone-plume complex.

Back Plume (Area-5)- Sandstone development within this zone illustrates the results of storm activity and/or transgression and the accompanying onshore reworking of the shelf sand plume. Spontaneous potential logs from this area (Fig. 17b) indicate that these deposits are composed of several thin (2-5 ft; .6-1.5 m) distinct sandstone bodies which attain net thicknesses of 8-25 ft (2.5-7.5 m). The numerous interbedded shale partings are thought to represent suspension sedimentation between periods of storm-induced sand deposition and may reduce reservoir communication and fluid migration. The up-dip location and the presence of

the landward mud seal, deposited by the entrapped eddy system (Figs. 6 and 14a-d), created favorable conditions for the stratigraphic trapping of hydrocarbons in these sandstones. The exploration potential for this area is believed to be fair to good.

The evolution of these sandstones is schematically shown in figure 17c. Lithologic characteristics which affect the hydrocarbon exploration potential and reservoir parameters reflect the depositional processes that were dominant within each of the subfacies.

Storm-Modified, Onshore-reworked Shelf Sand-Plume

The A1-3 shelf sandstone complex was used as the model for an onshore-reworked shelf sand-plume. The Navarro 'A' sandstone belt has been divided into three areas based on unique log response characteristics (Fig. 18a). Representative well logs for each of these areas (Fig. 18b) and a schematic representation of the sand-plume development is also shown (Fig. 18c).

Depocenter and Proximal Plume (Area-1)- Sandstones within this area represent deltaic, delta front and proximal sand-plume deposits. Electric logs of these sandstones (Fig. 18b) indicate that they are a sequence of several, 5-15 ft (1.5-4.5 m) thick, stacked frontal splays down-dip from the 60 ft (18 m) thick deltaic sandstones of the North Milam 'A' depocenter. This close association and lateral continuity between the proximal shelf-plume sandstones and the up-dip deltaic deposits, near the Kemp outcrop belt, is not conducive to the trapping and accumulation of hydrocarbons unless faulting interrupts up-dip fluid migration.

Seaward Margin (Area-2)- These sandstones represent the older, more

FIGURE 18. - Storm modified, onshore-reworked shelf sandstone-plume - A. A1-3 net sandstone map showing example electric log locations. Well Names - 1. Oleum Inc., Graham B-1, 6N-26E-8; 2. Jordan Drilling Co., Hitchcock #1, 5N-36E-1; 3. Combustion Products, Corp., Trimm #1, 5N-36E-5; 4. Inland Ocean, Inc., Baldwin #1, 5N-26E-1; 5. J. A. Leonard, Flentge #1, 5N-26E-4; 6. Prairie Prod. Co., #1 Marburger, 3N-25E-2. **B.** Selected electric log patterns. **C.** Plume evolution. **D.** Inferred estimates of hydrocarbon potential. Poor = 1; Excellent = 5.

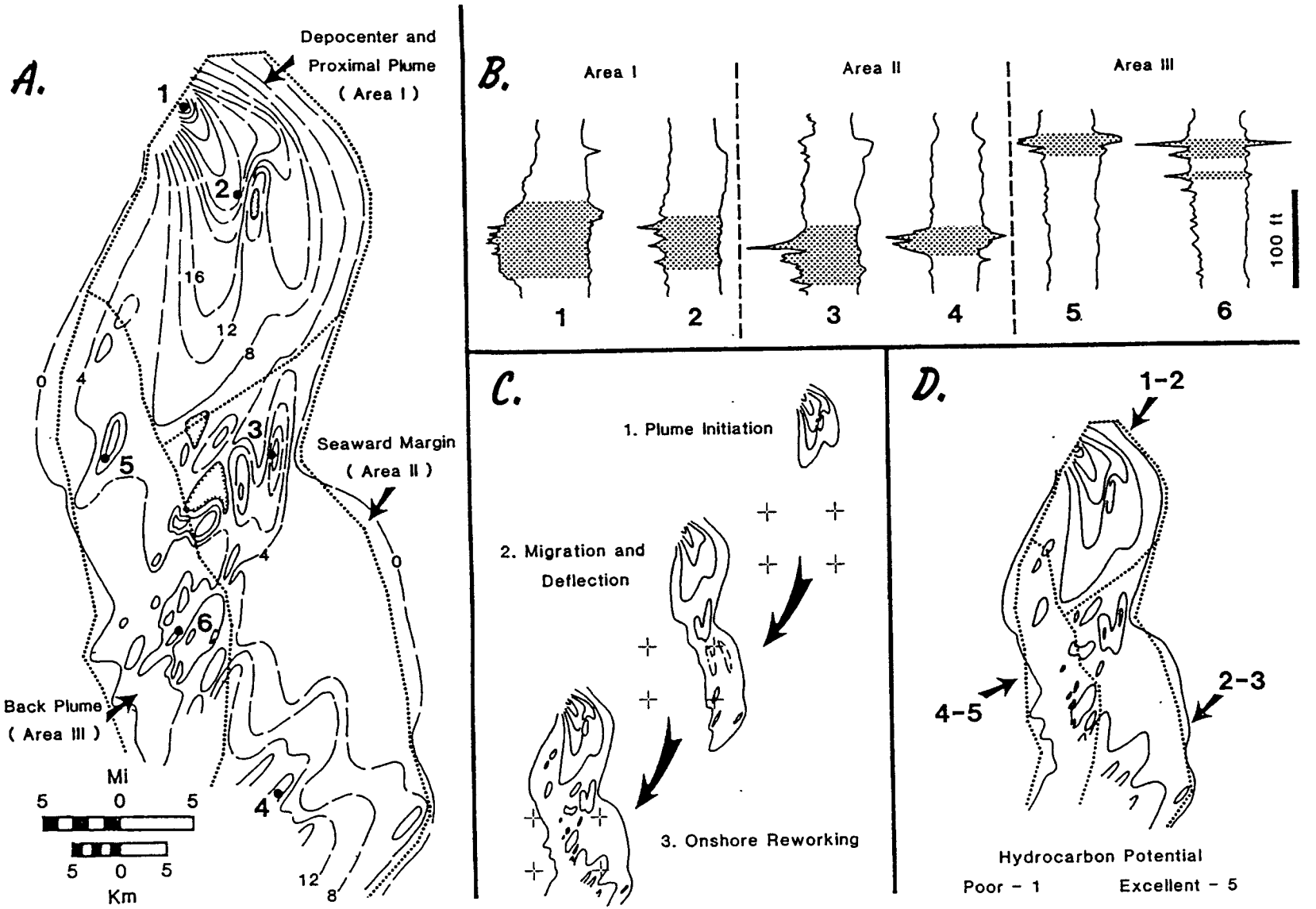
A.
Depocenter and
Proximal Plume
(Area I)
Seaward Margin
(Area II)
Back Plume
(Area III)
Mi
5 0 5
5 0 5
Km
B.
Area I
Area II
Area III
100 ft
1
2
3
4
5
6
C.
1. Plume Initiation
2. Migration and
Deflection
3. Onshore Reworking
D.
1-2
2-3
4-5
Hydrocarbon Potential
Poor - 1
Excellent - 5

basinward deposits of the Navarro 'A' shelf plume. The transition from the deltaic and proximal plume deposits to the sandstones of the plume's seaward margin is rather ill-defined and the boundary between these areas is somewhat arbitrary. The seaward margin of the sand-plume has several (1-5) fairly thick (5-15 ft; 1.5-4.5 m) sandstones which decrease in number while increasing in individual thickness down-current. The sandstones in the down-current, or distal, portion of the plume exhibit a 'coarsening-upward' spontaneous potential log pattern similar to migrating shelf-bar sandstones described by Berg (1975), Spearing (1976), and Boyles and Scott (1982), (Fig. 18b). The spatial distribution of the Navarro 'A' sandstones suggest that their deposition was heavily influenced by the configuration of the shelf and by the relief inherited from previous shelf depositional systems in particular. Hydrocarbon production from these stratigraphically deeper sandstones is rather limited and consists primarily of gas.

Back Plume (Area-3)- This area represents the up-dip limit of the Navarro 'A' sandstone plume. Onshore reworking of the seaward margin sands over the B1-4 shelf platform by transgressive, storm and fair-weather shelf processes resulted in the deposition of the stratigraphically isolated back plume sand bodies (Figs. 8b and 14g-h). These back plume deposits contain numerous (2-7) sandstone horizons which range in thickness from 2-10 ft (.6-3.0 m) and are separated by interbedded shales. These isolated sandstone bodies, located along the landward margin of the shelf sandstone plume, form ideal stratigraphic traps and consequently have a very high hydrocarbon potential.

CONCLUSIONS

Examination of subsurface data has facilitated the delineation of sandstone distribution patterns within the Kemp Clay of the Navarro Group (Maestrichtian) in east central Texas. Interbedded shales within the sandstone complexes has permitted the mapping of genetically related sandstone intervals and the reconstruction of a detailed depositional history for the system. Several of the more significant findings include the following:

(1) Micro-fossils associated with these sandstones indicate deposition occurred in a mid- to outer shelf environment.

(2) The mechanism for introduction of the sands onto the mud-rich shelf was the seaward deflection of southwestward flowing coastal/shelf currents. A modern analog for this has been documented on the Sinai Shelf east of the Nile River delta by Coleman et al, (1981).

(3) The sand transported by these paleocurrents formed elongate, arcuate shelf sand-plumes that were 17-20 mi (22-30 km) wide, extended 27-30 mi (44-46 km) downdrift, and at least 21-40 mi (34-64 km) into the basin. Thicknesses varied from 3-20 ft (1-6 m).

(4) Four distinct shelf sandstone-plumes were recognized within the study area. Sandstones within several of these plumes were stacked and redistributed by various shelf processes forming larger, 10-25 ft (3-7.6 m) thick plume complexes (Figs. 9 and 12).

(5) Log response characteristics within a sandstone-plume vary with relative plume position and permit the development of a generalized depositional model. These characteristics suggest that the clean sands

developed in the up-current portions of the plume due to prolonged winnowing by shelf currents. Shale content and numbers of shale partings increase with distance from the deltaic source.

(6) Thickness variations within individual plumes suggest significant differences in the surface morphology of the sand-plumes. Individual bars were stacked and concentrated into elongate ridges which exhibit a change in long axis orientations, from dip to strike oriented, with increasing distance down-current from the deltaic source (Figs. 9, 12 and 17).

(7) Distribution and characteristics of successive sand-plumes and plume complexes were influenced by previously deposited sand-plumes. Deposition of younger, basinward-accreting wedges of shelf deposits was, in part, controlled by the depositional topography inherited from older, underlying shelf/slope systems (Figs. 9, 12, and 14).

(8) Three distinct types of sandstone-plumes were recognized in the study area. These plume variants exhibit morphologies and lithologic characteristics (inferred from electric log responses) which reflect the processes dominant on the shelf at the time of their deposition.

(a) Rapidly-deposited, immature shelf sand-plume - This basic plume type represents the initial influx of siliciclastic material into the shelf environment. Rapid deposition and a short period of current and storm reworking contribute to its poorly-winnowed, shaley nature. Hydrocarbon exploration potential is confined to the cleaner sandstones of the proximal plume and seaward margin (Fig. 16).

(b) Abandoned, current-reworked shelf sand-plume - This current-modified plume complex is somewhat more complicated in its

depositional history and lithologic distribution with sand being reworked down-current and onshore. This variant has several areas of potential hydrocarbon accumulation including the deltaic depocenter, the proximal plume sheet sandstones, and the stratigraphically isolated distal and back plume areas (Fig. 17).

(c) Storm modified, onshore-reworked shelf sand-plume- Onshore reworking of this shelf sand plume resulted in the preservation of thin, stratigraphically isolated sand bars which climb stratigraphically onshore and down-current. These back plume shelf bars represent potentially very prolific hydrocarbon reservoirs (Fig. 18).

These stratigraphically isolated shelf sandstones, which are encased in orgainic rich maring shale, form almost ideal stratigraphic traps. A detailed understanding of shelf sand-plumes should provide a basis for efficient exploitation of potentially economically significant hydrocarbon deposits.

APPENDIX A

NAMES OF ELECTRIC LOGS USED IN THIS STUDY

Wells are arranged by tobin grid and section.

3N24E

3 Hunt Oil Co., Melcher #1
Hunt Oil Co., Patschke #1
4 Brazos Oil & Gas Co., Brade #1
8 Sun Oil Co., Melde #1
9 Union Oil Co. of California, L. E. Wells #1

3N25E

2 Prairie Producing Co., #1 Marburger
3 R. E. Haas, Fields #1

3N27E

1 Dugger & Herring, Weiler #1
TIPCO, Stern #1
3 Champlin Petroleum, Zgabay #1
TIPCO, Lamb #2

3N28E

3 C. R. B. Oil & Gas, Inc., Harris #2

4N24E

5 Taylor F. Refining Co., Milner #1
6 United North and South Dev. Co., Baine #1
9 Sutton Drilling Co., Fisher #1

4N25E

1 Phillips Petroleum Co., Smith AA-1
2 Lambert Hollub, Brown #2
Humble Oil & Refining, Vice #2
3 Kragseth, Brown #1
Shell Oil Co., Brown #2
5 Mustang Oil Co., Harzke #1
6 Amoco Prod. Co., Peebles #1
8 Pan American Petroleum Corp., Carlisle #1
K. P. Exploration, Carlisle #1
9 Standard Oil Co. of Texas, Biggers #1

4N26E

1 Inland Ocean Inc., Baldwin #1
3 Lambert Hollub Drilling Co., Chapman Unit #1
5 Maresh & Billingsley Oil Co., Orak #1
6 Marshall Exploration, Inc., Schmidt #1
7 Hill International Prod. Co., Baron #1
American Delta Corp., Koeppen #1
Champlin Petroleum Co., C. P. C. #1 Raymond Zboril
9 C. A. G. Petroleum Corp., Spacek #1

4N27E

2 C. A. G. Petroleum, Sand #1
Martin Oil & Gas, Norville #1
3 Columbia Oil & Gas, Goodnight #1
4 Adobe Oil & Gas Corp., E. Beran Unit #1
Strata Energy, Inc., Gerland #1
Strata Energy, Inc., Maresh #1
Champlin Petroleum Co., W. F. Eberhardt #1
6 C. A. G. Petroleum Co., Knesek #1
Columbia Gas & Development Corp., G. Gaas #1
7 TIPCO, Bohacek #1
8 TIPCO, Weichert #2
Champlin Petroleum Co., L. Kochler Unit #1
9 Champlin Petroleum Co., C. P. C. #1 A. Faust
Champlin Petroleum Co., G. Eberhardt

4N28E

2 Geodynamics Oil & Gas, Mais #1
Geodynamics Oil & Gas, Juries #1
3 C. P. C. Exploration Inc., Bird #1
4 C. A. G. Petroleum Co., Lauderdale #1
8 C. A. G. Petroleum Co., Karisch #1
9 Columbia Gas & Development Corp, Piwonka #1
Champlin Petroleum, Knesek A-#1

5N23E

7 Hamman Oil & Refining, McWilliams #1
B. R. Rose, Cumley #1

5N24E

2 Phillips Petroleum Co., Fitzgerald #1
4 C. H. Phifer, M. A. Porter #1
6 Ernest Oil Co., Harris #1

5N25E

1 General Crude Oil Co., Coffield #1
Mutual Oil of America, Payne #1
Brown & McKenzie, P. Perry #1
Brown & McKenzie, H. H. Coffield #1
J. A. Leonard, Kennedy Est. #1
White Shield Oil & Gas, D. H. Perry #1
J. A. Leonard, Coffield Unit #1
J. A. Leonard, Coffield 1-B
Mutual Oil of America, Grobener-Payne Unit #1
Mutual Oil of America, Wm. Payne #2
J. A. Leonard, Coffield 1-A
J. A. Leonard, Coffield 1-C
Brown & McKenzie, D. Scott 1-A
Danbert Oil & Gas, C. Avery #1

5N25E (continued)
J. A. Leonard, D. Scott 1-A
J. A. Leonard, Coffield #1
J. A. Leonard, Coffield #2
J. A. Leonard & Teten, Coffield #5
3 J. A. Leonard, Coffield Wright Unit #1
J. A. Leonard, Coffield Cook Unit #1
Texas Land & Trading, #2 Noack
T. Brown, #2 Orr
Coleman-Musselman, Prewitt #2
United Production Co., #3 Noack
4 Eaglerock, Luedgue #1
5 S. H. Rosenthal, L. Allen #1
Cabot Corp. H. Coffield
Ka-Hugh Enterprises, Crittenden #2
Ka-Hugh Enterprises, Crittenden #1-A
Ka-Hugh Enterprises, Morton #1
Ka-Hugh Enterprises, Cotton #4
Ka-Hugh Enterprises, Alford #1
Ka-Hugh Enterprises, Burroughs-Coffield #1
Ka-Hugh Enterprises, Cotton #1
Ka-Hugh Enterprises, Cotton #2
J. A. Leonard, Burney #2
Keese & Thomas, Miller #1
First United Oil & Gas, C. Willard #1
Lambert Hollub, Duncan #1
6 Brown & McKenzie, L. N. Avery
Texas Land & Trading, Burleson Oil #1
Texas Land & Trading, McGinnty-Avery #2
Texas Land & Trading, Bowers #1
Production Enterprises, Scott #1
Texas Land & Trading, Coffield #1
R. Teten, Coffield #7
Brown & McKenzie, C. N. Avery #1-A
Texas Land & Trading, McGinnty-Avery #1
Texas Land & Trading, McGinnty-Avery #3
Texas Land & Trading, McGinnty-Avery #4
Bowers, Ralston, Unit #3
J. A. Leonard, Russel #1-A
W. H. Wood, Russell #1-A
R. C. Burns, Cooksey #1
First United Oil & Gas, Varner #1
A. B. Alkek, K. K. Harrison #1
W. Wood, Dors #1
Bar-Mac, Morton #1
Bar-Mac, et al., Morton #2
J. A. Leonard, Cooksey #2
Bar-Mac, P. Holmes #1
Seagull Operators, Coffield B7B1

5N25E (continued)
Caddo Oil Co., Sheppard #1
Caddo Oil Co., Coffield B51A
Seagull Operators, Willard #1
Bar-Mac, et al., L. Morton #3
Bar-Mac, et al., L. Morton #6
Bar-Mac, et al., L. Morton #4
7 Caddo Oil Co., Coffield B7A #2
Caddo Oil Co., Coffield B7A #5
Challenge Oil & Gas, Cowden #1
J. A. Leonard, Coffield Smith F3
Lambert Hollub, Arledge #1
Lambert Hollub, #1 Willard Williams
Lambert Hollub, Key #1
Caddo Oil Co., Key #1
Lambert Hollub, J. Morton #3
Lambert Hollub, Willard #1
Lambert Hollub, Key #2
Lambert Hollub, Lina #1
Lambert Hollub, Poole #4
General Production, Wm. Willard #7
G. Rousseau, Powell #1
8 J. A. Leonard, Burney #1
Mutual Oil of America, Owen #1
Lambert Hollub, Coffield-Smith #2
Mutual Oil of America, Coffield #2
Mutual Oil of America, Coffield #1
McCarthy, Guthrie #1
McCarthy, Guthrie #2
Bar-Mac, # Gerdes Development
Carter Taylor, Nieto #1
Lambert Hollub, Coffield #3
Humble, First National Bank of Dallas #1

5N26E
1 Jordan Drilling Co., Hithcock #1
2 A. C. Hope, G. Heim #2
Caddo Oil Co., Black #3
Texas Land & Trading, G. Morse #1
Caddo Oil Co., Wendt #1
Caddo Oil Co., Speckman #2
Caddo Oil Co., Speckman #5
Hammill, Dobbins Est. #1
Caddo Oil Co., Boedecker #1
Caddo Oil Co., Murr #1
3 J. M. Huber, W. P. Hogan #1
J. M. Huber, W. P. Hogan #2
W. Holloway, H. Coffield #1
Caddo Oil Co., Coffield M-19

5N26E (continued)
General Crude, Perry #2
Texas Land & Trading, Coffield 2m
Caddo Oil Co., Coffield B-11, #3
J. A. Leonard, Coffield-Shaw Unit #2
M. Womack, H. H. Coffield #1
J. A. Leonard, Coffield et al. #1
General Production, F. Ryan #1
Texas Land & Trading, Robbinson #1
Texas Land & Trading, Raymond #2
Caddo Oil Co., Robbinson #1
Seagull Operating Co., Coffield B-10-3
J. A. Leonard, Coffield-Shaw #1
M. Womack, J. M. Fagan #1
General Production, Simpson #1
General Production, M. Caperton #1
General Production, L. Ryan #1
J. A. Leonard, Coffield D-3
General Production, Jones-Lewis #2
M. Womack, Jenkins #1
J. A. Leonard, Coffield-Winston C-1
Mutual Oil of America, J. Martin #1
Luling Oil & Gas Co., Martin #4-A
4 J. A. Leonard, Russell 3-B
J. A. Leonard, Coffield-Smith F-2
General Production, Jones Lewis #1
J. A. Leonard, Coffield-Winston A-2
J. A. Leonard, Coffield-Winston B-1
J. A. Leonard, Coffield-Winston C-2
J. A. Leonard, Russell 2-B
J. A. Leonard, Russell 1-B
J. A. Leonard, Cooksey 3-A
J. A. Leonard, Cooksey 2-A
J. A. Leonard, Roddy #2
J. A. Leonard, Coffield-Winston A-4
J. A. Leonard, White #1
J. A. Leonard, Coffield-Smith D-1
J. A. Leonard, Coffield-Smith C-1
J. A. Leonard, Smith, Coffield B-1
J. A. Leonard, Coffield-Smith A-1
J. A. Leonard, Coffield-Winston A-3
J. A. Leonard, Coffield-Winston A-1
General Production, O. F. Johnson #2
J. A. Leonard, Varner-Wendler Unit #1
Seagull Operating Co., Coffield B-4
J. A. Leonard, Coffield-Smith E-1
J. A. Leonard, Coffield-Smith F-1
General Production, O. F. Johnson #1

5N26E (continued)
J. A. Leonard, Coffield-Smith F-4
Lambert Hollub, Corsicana National Bank #1
General Production, Corsicana National Bank #1
General Production, D. Lednicky #1
J. A. Leonard, Flentge #1
J. A. Leonard, Coffield-Smith F-5
J. A. Leonard, Coffield-Smith E-2
General Production, Holliman #3
5 Lambert Hollub, Garr #1
Lambert Hollub, Price #1
Lear Petroleum Corp., Haish #1
Combustion Products, Trimm #1
8 Texas Gas Exploration, Sanders #1
General Production, Marek Unit #1
General Production, Beckman #1
General Production, Peck #1
General Production, T. A. Peek #1
General Production, M. B. East #1
General Production, W. O. Flentge #1
General Production, T. A. Peek A-1
9 General Production, Anderson #2
General Production, Holliman #2
General Production, Anderson #4
Caddo Oil Co., Key #3
Lambert Hollub, Willard #2
Lambert Hollub, Willard #3
Lambert Hollub, E. R. Willard #1
Lambert Hollub, Poole #3
J. A. Leonard, Pillow #1
J. A. Leonard, Pillow #2
J. A. Leonard, Pillow #3
J. A. Leonard, Pillow #5
Ferguson, Pillow #1
General Production, Rosenthal #2
Lambert Hollub, Poole #2
Lambert Hollub, Poole #6
Lambert Hollub, Poole #9
Lambert Hollub, Arledge 1-A
Lambert Hollub, Poole #10
Lambert Hollub, Tarwater #1
General Production, E. Arledge #1
General Production, F. Lina #1
General Production, Steinmeyer #1
General Production, A. Nelson #1
General Production, Dudley Unit #1
General Production, Pillow #1
General Production, Legg Unit #1

5N27E
1 Hemmingway, Telg #1
7 Strata Energy, Inc., Matcek Unit #1
Strata Energy, Inc., Slovacek #1

5N28E
1 C. P. C. Exploration, Scamardo Unit #1
2 Geodymanics Oil & Gas, Patterson #1
Dynamic Production, Jackson #1
7 Coffman, Tunis 4-#1
8 C. P. C. Exploration, McKinney #1
Fargo Energy Corp., Cleveland #1
9 C. P. C. Exploration, Matek #1

6N24E
1 M & M Oil Co., Lucas #4
Davis, Menke #1
6 R. Bradford, Black #2
Waterloo Oil Co., Brockenbusch #A-2

6N25E
1 Mustang Petroleum Co., Calloway #1
Behring Production, Inc., Lutner #1
2 K & H Operating Co., Dukes #3
W. F. Glenn, O'Neal #1
Texas Gulf Sulfur Co., Baker #1
R. Bradford, Labay #3
Anderson Brothers Corp., S. Miller #1
Davis, Smith, et al. #1
3 Caddo Oil Co., Coffield M-34-B-#1
4 Coleman-Head, S. C. Bland #1
Roundtree, Yoakum #1
7 Houston Petroleum, J. V. Kohut
9 Seagull Operating Co., Germanicus-Ryan #1
Texas Land & Trading, Lewis #1

6N26E
1 W. M. Galloway, Bornorden #1
Caddo Oil Co., Southwest Land No. 1
A. B. Rutland, Talafuse #1
W. M. Galloway, Fussell #1
2 Barge Oil & Gas, Inc., Henderson Est. #1
Caddo Oil Co., Coffield M-1c "A" (T-484-1) #1
Byrd Oil, W. A. Smith #1
Coastal Trend Oil Corp. et al., Norman #1
3 Coffield & Hardin, Holland #1
Taylor Refining Co., Batte #2
Martin Oil & Gas, C. White #1
Taylor Refining Co., Holdiness #1

6N26E (continued)

4 Midway Oil Corp., Genisk #1
Florence Elmer Trust, #1 Simmons
Houston Petroleum Co., #1 S. E. McGregor
Martin Oil & Gas, Hugh Stuart #2
Caddo Oil Co., Pearson (T-431-2) #1

5 D. M. Thomas, Bailey #1
Caddo Oil Co., Beard (T-535) #1-A
F. L. Gaines, Beard #1
Byron Rose, Page #1

7 Shell Oil Co., Newton #1

8 Oleum, Inc., Graham #B-1
Luling Oil & Gas Co., #E-1 Coffield
Caddo Oil Co., Rockdale State Bank 1-A
A. C. Hope, E. L. Hana

9 J. M. Huber Corp. et al., R. Love #1
Houston Petroleum Co., #1 E. Love
Caddo Oil Co., Krueger #1
Caddo Oil Co., Rockdale State Bank #1
Shane Oil Corp., J. Martin #1
Crestmont Oil & Gas, Blackburn #1
Mutual of America, Roach-Jackson
Luling Oil & Gas, Caldiron #2
Varn Petroleum Co., H. L. Christie Est.

6N27E

3 Shell Oil Co., Nell Ross #1

4 Shell Oil Co., Adoue Est. #1

5 D. Wagner & Co., Oxsheer Smith #2

8 Scurlock Oil, Clanton #1

7N25E

2 Stroube Drilling Co., Short #1

5 J. W. Williams, A. Bickett #1
C. T. Grubbs, Lamkin #2
Pemberton, Lamkin #3
R. G. Rice, Culpepper #1
W. C. Pemberton, McLerran #1

7 Anderson Brothers Corp., Turney #1
B. J. Taylor, Young & Baty #1

8 Austral Oil Co., Angell No. 1-W
Olen Oil Co., McCormick #5

9 B. J. Taylor, Kubiak #A-2

7N26E

1 Exxon, Foster #1

2 TIPCO, J. Smoot #1

5 Pemberton Co., J. Robinson #1
TIPCO, McDaniels #1

7N26E (continued)
Byrd Oil Co., Henderson #1
6 Standard Oil of Texas, C. E. Smith #1
7 Byrd Oil Co., Greene #2
8 Martin Oil & Gas Co., V. Ashley #1
Anderson Brothers Corp., L. York #1
9 Seagull Operating Co., R. Conner #1
Anderson Brothers Corp., Ashley #1

7N27E
9 Pemberton Co., #1 Hardcastle
B&B & WCP, Hardcastle #1

7N28E
9 Geodynamics, Reistine #1

8N25E
1 Rimrock Tidelands, Crawford #1
6 Bighart Oil & Gas, Kennon #1
9 B. H. Vick, Denco #1
Bighart Oil & Gas, Glady's York #1

8N26E
1 D. A. McCrary, Morris #2
C. A. Williams, Patzke #1
6 Hamman Oil & Refining, Gibson #1
Hamman Oil & Refining, Patzke #1
Hammon Oil & Refining, Gibson #2
Febecco Oil corp., Gibson Unit #1

8N27E
5 T. O. Posey, Weber 1-A
9 Standard Oil Co. of Texas, A. I. Smith #1
Placid Oil Co., Eva Smith #1

8N28E
6 Humble, Michael #1

9N25E
6 West & Smith, White Est. #1

9N26E
4 L. M. Josey, Gerdes #1
Prime Petroleum Co., Ellison #1-A
Production Service, Ellison Bros. #1
Kelley-McGregor, Ellison Bros. #1
8 W. A. Bryan, Hyde #1
9 O. B. Siler, Askew #1

9N27E
6 Dallas Exploration, Lutz #1
7 Union Production Co., Wiese #1
Darant & Graham Oil Co., Fagan #1
8 N. G. Penrose, Inc., Ables #1
9 W. H. Doran, Woodall #1
A. G. Hill, Anderson #1

9N28E
2 G. I. Warren, Nash #1

10N26E
1 Paul White, Kelly #1

10N27E
6 B. Manziel, Lastor #1-A
7 Magnolia Petroleum Corp., Koperczak #1

10N28E
3 Lyons Petroleum, Inc., Anchicks & Nickelson #1
4 B. B. Orr, Abraham #3
Brelsford, Hemphill & Irwin, Allen #B-1
9 McHenry, Abraham #1

REFERENCES

Adkins, W. S., 1932, The Mesozoic systems in Texas, in E. H. Sellards, W. S. Adkins, and F. B. Plummer (eds), The geology of Texas: University of Texas Bull., no. 3232, 2nd printing, p. 239-519.

Anderton, R., 1976, Tidal shelf sedimentation: an example from the Scottish Dalradian: Sedimentology, v. 23, p. 429-458.

Asquith, D. O., 1970, Depositional topography and major marine environments, Late Cretaceous, Wyoming: AAPG Bull.,v. 54, p. 1184-1224.

_____, 1974, Sedimentary models, cycles, and deltas, Upper Cretaceous, Wyoming: AAPG Bull., v. 58, p. 2274-2283.

Barratt, J. C., 1982, Fales Member (Upper Cretaceous) deltaic and shelf-bar complex, central Wyoming: unpub. M.A. thesis, Univ. of Texas at Austin, 120 p.

Bates, C. C., 1953, Rational theory of delta formation: AAPG Bull., v. 37, p. 2119-2162.

Belderson, R. H., and A. H., Stride, 1966, Tidal current fashioning of a basal bed: Marine Geol., v. 4, p. 237-257.

Berg, R. R., 1975, Depositional environment of Upper Cretaceous Sussex Sandstone, House Creek field, Wyoming: AAPG Bull., v. 59, p. 2099-2110.

Boyles, J. M., and A. J. Scott, 1982, A model for migrating shelf-bar sandstones in Upper Mancos Shale (Campanian), northwestern Colorado: AAPG Bull., v. 66, p. 491-508.

Brenner, R. L., 1978, Sussex sandstone of Wyoming - example of Cretaceous offshore sedimentation: AAPG Bull., v. 62, p. 181-200.

Caston, V. N. D., 1972, Linear sand banks in the southern North Sea: Sedimentology, v. 18, p. 63-78.

Coleman, J. M., H. H. Roberts, S. P. Murray, and M. Salama, 1981, Morphology and dynamic sedimentology of the eastern Nile delta shelf, in C. A. Nittrourer, (ed), Sedimentary dynamics of continental shelves: New York, Elsevier, p. 301-326.

Field, M. E., 1980, Sand bodies on coastal plain shelves: Holocene record of the U.S. Atlantic inner shelf off Maryland: Jour. Sed. Petrology, v. 50, p. 505-528.

_____, C. H. Nelson, D. A. Cacchione, and D. E. Drake, 1981, Sand waves on an epicontinental shelf: northern Bering Sea, in C. A. Nittrourer (ed), Sedimentary dynamics of continental shelves: New York, Elsevier, p. 233-258.

Fisher, W. L., L. F. Brown, Jr., A. J. Scott, and J. H. McGowen, 1969, Delta systems in the exploration for oil and gas: a research colloquium: Univ. of Texas, Bur. Econ. Geology.

Flemming, B. W., 1980, Sand transport and bedform patterns on the continental shelf between Durban and Port Elizabeth (southeast African continental margin): Sedimentary Geol., v. 26, p. 179-205.

_____, 1981, Factors controlling shelf sediment dispersal along the southeast African continental margin, in C. A. Nittrourer, (ed), Sedimentary dynamics of continental shelves: New York, Elsevier, p. 259-277.

Hagar, D. S., I. O. Brown, 1924, The Minerva oil field, Milam county, Texas: AAPG Bull., v. 8, p. 632-640.

Hamblin, A. D., and R. G. Walker, 1979, Storm-dominated shallow marine deposits: the Fernie-Kootenay (Jurassic) transition, southern Rocky Mountains: Canadian Jour. Earth Sciences, v. 16, p. 1673-1690.

Hayes, M. O., 1967, Hurricanes as geologic agents: case studies of hurricanes Carla, 1961, and Cindy, 1963: Texas Univ. Bur. Econ. Geology, Rept. Inv. No. 61, 56 p.

Hill, R. T., 1901, The geography and geology of the Black and Grand Prairies of Texas: U.S. Geol. Survey, 21st Ann. Rept., pt. 7, 666 p.

Hobson, J. P., Jr., M. L. Fowler, E. A. Beaumont, 1982, Depositional and statistical exploration models, Upper Cretaceous offshore sandstone complex, Sussex Member, House Creek field, Wyoming: AAPG Bull., v. 66, p.689-707.

Houbolt, J. J. H. C., 1968, Recent sediments in the Southern Bight of the North Sea: Geol. Mijnbouw, v. 47, p. 245-273.

Kenyon, N. H., 1970, Sand ribbons of European tidal seas: Marine Geology, v.9, p. 25-39.

Kreitler, C. W., et al, 1980, Geology and geohydrology of the East Texas Basin: a report on the progress of nuclear waste isolation feasibility studies (1979): Univ. of Texas, Bur. Econ. Geology Geologic Circular 80-12, 112 p.

_____, 1981, Geology and geohydrology of the East Texas Basin: a report on the progress of nuclear waste isolation studies (1980): Univ. of Texas, Bur. Econ. Geology Geologic Circular 81-7, 207 p.

McCave, I. N., 1971, Sand waves in the North Sea off the coast of Holland: Marine Geol., v. 10, p. 199-225.

McGowen, M. K., and C. M. Lopez, 1981, Depositional systems in the Nacatoch Formation (Upper Cretaceous), northeast Texas and southwest Arkansas, in C. W. Kreitler, et al, Geology and geohydrology of the East Texas Basin: a report on the progress of nuclear waste isolation studies (1980): Univ. of Texas, Bur. Econ. Geology Geologic Circular 81-7, p. 60-68.

McManus, D. A., and J. S. Creager, 1963, Physical and sedimentary environments on a large spitlike shoal: Jour. Geol., v. 71, p. 498-512.

Nichols, R. H., G. E. Peterson, and C. E. Wuerstner, 1968, Summary of subsurface geology of northeast Texas, in B. W. Beebe and B. F. Curtis, (eds), Natural gases of North America: AAPG Memoir 9, v. 2, p. 982-1004.

Palmer, J. J., and A. J. Scott, in press, Stacked shoreline and shelf sandstones of the La Ventana Tongue (Campanian), northwest New Mexico: AAPG Bulletin.

Pessagno, E. A., Jr., 1969, Upper Cretaceous stratigraphy of the western Gulf Coast area of Mexico, Texas, and Arkansas: Geol. Soc. America Memoir 111, 139 p.

Pilkey, O. H., and M. E. Field, 1972, Onshore transportation of continental shelf sediment: Atlantic southeastern United States, in D. J. P. Swift, D. B. Duane, and O. H. Pilkey, (eds), Shelf sediment transport: process and pattern: Stroudsburg, Pa., Dowden, Hutchinson, and Ross, p. 429-446.

Pikley, O. H., et al, 1981, The Georgia Embayment continental shelf: stratigraphy of submergence: Geol. Soc. America Bull., v. 92, p. 52-63.

Porter, K. W., 1976, Marine shelf model, Hygiene Member of the Pierre Shale, Upper Cretaceous, Denver Basin, Colorado: Colorado School Mines Prof. Contr. no. 8, p. 251-263.

_____, and R. J. Weimer, 1982, Diagenetic sequence related to structural history and petroleum accumulation: Spindle field Colorado: AAPG Bull., v. 66, p. 2543-2560.

Spearing, D. R., 1976, Upper Cretaceous Shannon Sandstone: an offshore, shallow marine sand body: Wyoming Geol. Assoc. 28th Ann. Guidebook, p. 65-72.

Stephenson, L. W., 1927, Notes on the stratigraphy of the Upper Cretaceous formations of Texas and Arkansas: AAPG Bull., v. 11, p. 1-17.

_____, 1941, Summary of faunal studies of Navarro Group of Texas: AAPG Bull., v. 25, p. 637-643.

Stride, A. H., 1963, Current swept floors near the southern half of Great Britain: Quart. Jour. Geol. Soc. London, v. 119, p. 175-199.

Swift, D. J. P., 1975, Tidal sand ridges and shoal retreat massifs: Marine Geol., v. 18, p. 105-134.

_____, et al, 1971, Relict sediments, a reconsideration: Jour. Geology, v. 79, p. 329-346.

_____, et al, 1972, Holocene evolution of the shelf surface, central and southern Atlantic shelf of North America, in D. J. P. Swift, D. B. Duane, and O. H. Pilkey, (eds), Shelf sediment transport: process and pattern: Stroudsburg, Pa., Dowden, Hutchinson, and Ross, p. 499-574.

_____, et al, 1973, Ridge and swale topography of the Middle Atlantic Bight, North America: a secular response to the Holocene hydraulic regime: Marine Geol., v. 15, p. 227-247.

_____, et al, 1977, Holocene evolution of the inner shelf of southern Virginia: Jour. Sed. Petrology, v. 47, p. 1454-1474.

_____, and M. E. Field, 1981, Evolution of a classic sand ridge field: Maryland sector, North American inner shelf: Sedimentology, v. 28, p. 461-482.

Terwindt, J. H. J., 1971, Sand waves in the Southern Bight of the North Sea: Marine Geol., v. 10, p. 51-67.

Texas State Railroad Commission, 1983, Annual Report of the Oil and Gas Division, 1982: Austin, Texas.

Turner, J. R., and S. J. Congers, Environment of deposition and reservoir properties of the Woodbine Sandstone at Kurten field, Brazos county, Texas: Gulf Coast Assoc. Geol. Soc. Trans., v. 31, p. 213-232.

Vail, P. R., R. M. Mitchum, Jr., and S. Thompson, III, 1977, Seismic stratigraphy and global changes of sea level, part 4: Global cycles of relative changes of sea level: AAPG Memoir 26, p. 83-97.

The vita has been removed from the digitized version of this document.